Evolution of Cooperation under Environmental Variability

Masaaki Inaba

March 2026

Evolution of Cooperation under Environmental Variability

Graduate School of Science and Technology
Degree Programs in Systems and Information Engineering
University of Tsukuba

Masaaki Inaba

March 2026

Abstract

[TODO]

Contents

List of Figures

List of Tables

Chapter 1

Introduction

Cooperation is fundamental to human society. Some forms of cooperation support basic biological survival and reproduction, including cooperative hunting, resource sharing, collective defense against predators, and alloparental care. Others reflect uniquely human sociality, such as division of labor, gift-giving, exchange, knowledge transmission, and formation of alliances. The prosperity of *Homo sapiens* would have been impossible without these behaviors. However, the evolutionary origins of cooperation are not fully understood and have been actively studied from Darwin's era to the present day.

1.1 Theoretical background

Darwin's theory of natural selection in *On the Origin of Species* (1859) [1] includes the principle that nature favors traits that increase individual fitness—the ability for individuals to survive and reproduce. However, although cooperative behaviors, particularly altruistic ones, appear to enhance the fitness of others or the group rather than the actor's own fitness, such behaviors are widespread across diverse taxa, from microorganisms to social insects to mammals. If natural selection favors traits that increase individual fitness and cooperation appears to decrease individual fitness, why is cooperation so ubiquitous? Darwin himself recognized this paradox [2].

This puzzle was initially studied within evolutionary biology and was later taken up by a wide range of disciplines, including physics, economics, and psychology, eventually giving rise to an interdisciplinary field known as *the evolution of cooperation*. The following paragraphs review several key studies in the evolution of cooperation, highlighting their main contributions and limitations.

Hamilton (1964) [3, 4] introduced the concept of inclusive fitness to explain the evolution of altruistic behaviors among genetically related individuals and formalized this insight as Hamilton's rule. This theoretical framework provides a powerful explanatory principle for cooperation among kin across diverse taxa, from social insects to primates. However, Hamilton's rule, in its

original form, cannot explain altruistic behaviors between non-relatives, which are particularly prevalent in human societies. Recent attempts have been made to extend Hamilton's rule to general cooperation mechanisms beyond kin relationships, but the validity of these extensions remains debated [5–7].

Maynard Smith and Price (1973) [8] introduced evolutionary game theory, providing a mathematical framework for analyzing how behavioral strategies, including cooperation and defection, spread in populations. Their approach treats strategies as heritable traits subject to natural selection, allowing researchers to predict which strategies will persist in populations over evolutionary time. This framework has become fundamental to studying the evolution of cooperation, as it enables formal analysis of how cooperative and selfish strategies compete and coexist.

Axelrod and Hamilton (1981) [9] demonstrated that reciprocal cooperation can evolve among non-relatives through repeated interactions. Using the iterated prisoner's dilemma game, they showed that simple reciprocal strategies such as Tit-for-Tat, which cooperates initially and then mimics the opponent's previous action, can be evolutionarily successful when individuals interact repeatedly and can recognize their past partners. This work established direct reciprocity as a fundamental mechanism for the evolution of cooperation. However, this mechanism requires individuals to recognize each other and remember past interactions, making it applicable primarily to small groups with repeated encounters. In large-scale societies where interactions are often anonymous or infrequent, alternative mechanisms are needed to explain the prevalence of cooperation.

Addressing these limitations, Nowak and his collaborators advanced research on various mechanisms that promote cooperation, including indirect reciprocity [10, 11], network reciprocity [12], and group selection [13]. Building on these studies, Nowak (2006) [14] synthesized the theoretical developments in the field, proposing five fundamental mechanisms for the evolution of cooperation: kin selection, direct reciprocity, indirect reciprocity, network reciprocity, and group selection. This framework provided a comprehensive taxonomy for understanding how cooperation can evolve under different ecological and social conditions. However, Nowak's synthesis has been criticized as essentially reformulating Hamilton's rule in different contexts, as each of these mechanisms can be understood within the framework of inclusive fitness theory [15]. Moreover, while this taxonomy is useful for categorizing mechanisms, it does not address how these mechanisms interact or which conditions favor one mechanism over another in realistic ecological settings.

These theoretical developments have established fundamental frameworks for understanding cooperation. We can no longer naively say that cooperation is a mystery. However, these frameworks remain highly general and abstract. In recent years, research has increasingly shifted toward examining cooperation under more specific circumstances and mechanisms. These studies investigate how factors such as reputation, social norms, memory, complex network structures,

learning mechanisms, and environmental variability (EV) shape the evolution of cooperation. Such context-specific approaches complement the general theoretical frameworks and provide insights into the diverse forms of cooperation observed in nature and human societies.

Among these context-dependent factors, we focus on EV for two reasons. First, there is a hypothesis supported by empirical data suggesting that EV drove the evolution of uniquely human behaviors (*modern human behavior*), including cooperative behavior. However, the direct causal relationship between EV and cooperation remains unclear. Second, other factors such as networks, norms, and learning algorithms are actively researched because they directly influence cooperation. However, EV appears to be less directly related to cooperation, and thus has been studied less than other factors in the field of the evolution of cooperation. These two points are detailed in the following Sections 1.2 and 1.3.

1.2 Environmental variability and the evolution of modern human behavior

Modern human behavior refers to a suite of traits characteristic of *Homo sapiens*, including abstract thinking, symbolic expression, complex planning, language, art, and crucially, large-scale cooperation and ultrasociality. Numerous studies concur that these behavioral patterns emerged during the Middle Stone Age (MSA) in Africa [16–20]. While there is broad consensus on when and where these behaviors originated, the mechanisms driving their emergence remain enigmatic despite various proposed theories.

Among various hypotheses proposed to explain these developments, the variability selection hypothesis (VSH), proposed by Potts (1996, 1998) [21, 22], suggests that EV was a primary driving force in human evolution. According to this hypothesis, intensified environmental fluctuations during MSA in Africa favored "versatilists", those capable of rapid adaptation to new environments over "specialists", who adapt to specific environments, or "generalists", who adapt across a range of environments. In this context, EV encompasses changes in landscape dynamics (such as land-lake oscillations), climate fluctuations (such as arid-moist climate oscillations), variations in flora and fauna, ultimately leading to the unpredictability of resource availability.

Initially, this hypothesis was supported by a temporal correlation between intensified environmental changes, the replacement of human species, and the increased complexity of cultural artifacts, such as stone tools and ornaments [23]. In addition, the cognitive buffer hypothesis (CBH) [24–26] provides a neuroscientific basis for VSH, and a mathematical model [27] demonstrates its theoretical feasibility. The CBH posits that larger brain sizes in animals, including humans, evolved as a buffer against EV, enhancing survival through improved problem-solving and learning abilities. In contrast, several theories [28–30] propose that EV and behavioral

diversity do not necessarily drive human encephalization. These theories emphasize the role of social contexts, as suggested by the social brain hypothesis (SBH) [23, 31–37], and consider other factors such as dietary influences [38, 39]. The SBH argues that human intellectual abilities evolved in response to the selection pressures of complex social environments, which required the effective management of social relationships within and between groups.

While temporal correlations between EV and the emergence of modern human behavior are evident, the causal mechanisms remain debated. In particular, the fact that large-scale complex cooperation is a component of modern human behavior raises the question of whether EV also played a role in the evolution of cooperation. This speculative link provides the first motivation of this dissertation.

1.3 Environmental variability and the evolution of cooperation

Most previous studies on the evolution of cooperation have not considered environmental factors, assuming fixed environmental conditions. Nevertheless, a small but growing number of studies have examined cooperation under EV.

These works on EV can be broadly categorized into extrinsic EV models and intrinsic EV models. Extrinsic EV can be represented through several models, including fluctuations in the population that the environment can sustain [40, 41], stochastic variations in payoff matrices or game rules [42–44], variability in learning, and information transmission mechanisms [45, 46]. Differences in resource availability have also been studied [47], though the model does not involve temporal variability but rather compares static scenarios of abundance and scarcity. Intrinsic EV, in contrast, refers to EV in which interactions in a system modify the environment, and environmental feedback in turn shapes the system's behavior [48, 49].

While anthropogenic environmental change is increasingly critical in modern societies, such feedback effects would be negligible in the context of MSA. Therefore, we focus on extrinsic EV rather than intrinsic EV. This extrinsic EV should capture the unpredictability of resource availability, as explained in Section 1.2. Specifically, we examine how increased intensity of EV between abundant and scarce conditions affects evolutionary dynamics, rather than unidirectional shifts from abundance to scarcity or vice versa. This aspect of EV has not been previously studied, constituting our second motivation.

1.4 Research objectives and approach

Given the research gaps identified above, this dissertation addresses the following key research questions: (i) Does EV promote cooperation? and (ii) If so, how does it?

To address these research questions, we adopt a constructive approach. The constructive approach is a methodology that seeks to understand phenomena by artificially constructing systems that reproduce them and analyzing their behavior. In the context of this dissertation, we employ multi-agent simulations based on evolutionary game theory to reproduce and examine the evolutionary dynamics of cooperative behavior under EV.

We adopt this simulation-based approach for three reasons. First, directly observing evolutionary processes is infeasible because they occur over timescales far beyond experimental reach; simulations allow us to observe such dynamics within tractable timeframes. Second, simulations enable systematic manipulation of variables such as the intensity of EV, which cannot be controlled in natural situations. Third, simulations allow us to isolate causal relationships by simplifying conditions, whereas in the real world numerous confounding factors mediate the relationship between EV and cooperation.

However, this approach has inherent limitations. Because our simulations abstract away from the complexity of real systems, they cannot provide precise quantitative predictions, such as the specific magnitude of EV required to produce a given level of cooperation. Rather, our objective is to reproduce broad qualitative patterns and to identify the mechanisms through which EV can promote or hinder cooperation, providing theoretical insights that complement empirical research.

1.5 Organization

In this chapter, we reviewed the field of the evolution of cooperation, highlighting that while general theoretical frameworks have been well established, research examining cooperation under specific contexts remains an active area of investigation. We then identified the relationship between cooperation and EV as the central focus of this dissertation and posed two research questions: whether EV promotes cooperation, and if so, how. Finally, we introduced our simulation-based constructive approach to address these questions and clarified its scope and limitations.

Numerous approaches to modeling the evolution of cooperation under EV are conceivable. In this dissertation, we consider three abstract models, examined in Chapters 2, 3, and 4. Given this diversity of possible approaches, these models are not exhaustive, yet they provide an important starting point for future theoretical and empirical research.

Chapter 2 (The base model) introduces a base model that examines the evolution of cooperation among geographically distinct groups under EV. In this model, groups represent sites at which resources may concentrate, such as riverbanks or lakeshores, where human populations naturally gathered. A limitation of this model is that it does not account for migration between groups.

Chapter 3 (The 2-level model with migration) extends the base model by introducing a

two-level structure with individual-level migration. Here, each geographical group, as defined in Chapter 2, contains multiple individuals who can move between groups. This framework allows us to examine how EV influences cooperation when individual migration is considered. However, while this model is a natural extension of Chapter 2, it represents a relatively unique approach within the existing studies on cooperation and migration, limiting comparability with prior works.

Chapter 4 (The 2-dimensional model with migration) addresses this limitation by employing a two-dimensional spatial structure, widely used in the literature on cooperation with migration. In this model, without assuming explicit group structures, as defined in Chapters 2 and 3, we investigate how EV influences cooperation among individuals moving across a two-dimensional space.

Chapter 5 (Conclusion) synthesizes the findings from the three models in Chapters 2, 3, and 4 to discuss the commonalities and differences in the mechanisms. We further consider the implications and significance of this research, as well as its limitations and directions for future work.

Finally, to provide an overall perspective, Table 1.1 summarizes the key concepts used throughout this dissertation, although some are formally described in later chapters.

Table 1.1: Key concepts used throughout this dissertation

Term	Description
Agent	An autonomous unit in simulation models that possesses a behavioral strategy, perceives its environment and takes actions. In Chapter 2, agents represent groups. In Chapter 3, two levels of agents exist: groups and individuals within groups. In Chapter 4, agents represent individuals.
Individual	An agent representing the unit of migration. Due to this definition, individuals are not necessarily single persons but may represent small groups such as families. In Chapter 2, individuals are not explicitly modeled. In Chapter 3, individuals migrate between groups. In Chapter 4, individuals migrate across a 2D space.
Group	A collection of individuals sharing a common geographical location. In Chapter 2, groups are modeled as agents. In Chapter 3, groups are modeled as high-level agents, incorporating individuals as low-level agents. In Chapter 4, groups are not explicitly modeled, though spatial clusters (i.e., spontaneous group-like structures) of individuals with the same strategy may emerge.
Cooperation	Altruistic behavior that appears to benefit other agents at a cost to the acting agent (i.e., individual or group). Cooperation (C) and its alternative behavior, defection (D), are used as behavioral strategies of an agent in game-theoretic models.
Environmental Variability (EV)	Temporal fluctuations in the spatial distribution of resource availability. This dissertation focuses on extrinsic EV, which occurs independently of human activity, reflecting unpredictable climate and landscape fluctuations during the MSA in Africa. In the later chapters, EV is modeled through the stochastic movement of Sources of Resources (SoRs), focal points of resource abundance, and the resulting shifts in resource distribution.
Migration and Mobility	Migration means spatial movement of individuals in response to resource availability or environmental conditions, while mobility means the ability to migrate. In Chapter 2, migration is not incorporated. In Chapter 3, individuals migrate between groups. In Chapter 4, individuals migrate across a 2D space.

Chapter 2

The base model

This chapter[1] introduces a base model to examine our research questions: whether and how environmental variability (EV) promotes the evolution of cooperation. Although migration is a reasonable response to EV for people during the Middle Stone Age (MSA), we exclude it here to focus on the direct effects of EV on cooperation. The combined effects of EV and migration are examined in Chapters 3 and 4.

2.1 Model

We use an agent-based simulation model within the framework of evolutionary game theory to investigate how increasing EV influences the evolution of cooperation. Given the limited availability of detailed data on EV and the spatial distribution of hominid groups during the MSA in Africa, our model adopts a highly abstracted approach, aiming to reveal the general effects of EV based on reasonable assumptions while excluding specific details. The model operates as follows: several geographically separated regions, each with varying levels of resource accessibility, experience fluctuating resource availability over time (EV). Each region hosts a single group (agent), and interactions between groups, such as resource exchanges (game) and behavioral pattern transmission (reformation), affect and adjust their relationships.

There are several points of concern when using the term "group". First, groups within the complex social environment described by the social brain hypothesis (SBH) are nested in a series of fractal-structured networks [37, 51, 52]. As a result, when smaller groups ally and cooperate to form a larger group, whether this cooperation is viewed as intragroup cooperation within the larger group or intergroup cooperation among the smaller groups depends on the level of analysis. For simplicity, we assume a certain level of grouping and analyze their intergroup cooperation, though this could alternatively be seen as intragroup cooperation from the perspective of a higher-level group. Furthermore, while treating groups as units of adaptation is highly debated in evolutionary biology [53–55], our focus here is on cultural evolution rather

[1] This chapter is based on Inaba and Akiyama (2025) [50], published in *PLOS Complex Systems*.

than biological evolution. In this cultural context, we assume that a group has a degree of autonomy, treating individual relationships and nested group structures as a black box. Here, autonomy suggests that the basic behavioral patterns for a group regarding which groups it cooperates with or does not are influenced by intergroup interactions and evolve over time.

Agent and structure

In this chapter, each agent represents a single group and has a strategy of either cooperation or defection ("C" represents a cooperation strategy or a cooperator, while "D" represents a defection strategy or a defector). Initially, all agents are set to D, as intergroup cooperation is considered extremely unlikely [56, 57]. This chapter focuses exclusively on intergroup interactions and does not consider intragroup interactions. While a two-level model would be necessary to analyze the tension between intergroup and intragroup interactions, as seen in multilevel selection studies, a one-level model is suitable here given our focus on intergroup interactions. All agents are situated within a geographic structure, forming an interaction structure.

The geographic structure is modeled as a line segment with periodic boundary conditions, represented visually as a circle (Fig 2.1). N agents are evenly spaced along the circle. Although a one-dimensional spatial structure is used for simplicity, more realistic structures can be explored as empirical studies progress. Migration is not considered in this chapter to keep the model simple as an initial approach. We incorporate migration in Chapters 3 and 4, as it is reasonable to assume that a group might move to a resource-rich region when its resources become scarce. However, the assumption of no migration is not entirely unrealistic, as some studies have highlighted the tendency for settlement during the MSA [58–60].

The interaction structure defines the relationships between agents, which are not limited by the geographic arrangement. These relationships affect the frequency of games (described later) and are subject to rewiring through reformations (also described later). The network, where agents are represented as nodes and relationships as edges, is characterized as an undirected, unweighted, and dynamic graph. The initial network is a regular network with a degree of $k = 4$.

EV

The resource represents the amount of goods or wealth necessary for survival that a group (agent) can obtain from the natural environment (e.g., food, materials for stone tools required to gather food). Resources are allocated to each agent at each time step, with the amount varying across different regions. The node with the highest resource allocation is referred to as the *Source of Resources* (SoR). The further an agent is located from the SoR geographically, the less resource it receives, as determined by the resource decrement factor, f_{RD}. Specifically,

the resource allocated to agent i is calculated as $r_i = r_p - |i - p| f_{RD}$. Here, r_i represents the resource allocated to agent i, p is the index of the SoR, and $|i - p|$ represents the distance between i and p, accounting for the boundary conditions, rather than the usual absolute value. Additionally, there is a universal resource threshold, θ, for all agents; any agent falling below this threshold must reformulate its strategy and relationships.

In this dissertation, EV refers to resource variability, represented by stochastic models. EV can be divided into variability in distribution of resources among regions and in total quantity of resources across all regions. Although variations in resource types are also an important consideration, we simplify the model assuming a single resource type. The two forms of variability are termed regional variability (RV) and universal variability (UV). RV is a type of EV in which the distribution of resource-rich and resource-poor regions changes over time; specifically, the SoR moves randomly. The SoR's index p_t at time t fluctuates according to a stochastic process expressed as $p_{t+1} = (p_t + \Delta_t) \mod N$. Here, Δ_t is a random integer step uniformly distributed within the range $[-\sigma_R, \sigma_R]$, where $0 \leq \sigma_R \leq N/2$. UV represents another form of EV in which the total resource quantity fluctuates randomly over time, while the resource distribution between regions remains fixed. This variability reflects large-scale fluctuations in resource availability across a wide area encompassing all regions. However, to simplify the implementation, we fix the resource values and instead model UV by varying the threshold value θ, which determines when reformation occurs. The fluctuation is modeled by a first-order autoregressive process, or AR(1) [61–63], $\theta_{t+1} = \mu_\theta(1 - \beta) + \theta_t \beta + \epsilon$ with $0 \leq \beta < 1$ and $\epsilon \sim N(0, \sigma_\theta^2)$, where μ_θ is the expected value of θ, β is the autoregressive coefficient, and ϵ is a normally distributed noise term with mean 0 and standard deviation (SD) σ_θ. The intensity of RV is determined by the shift range of the SoR (σ_R), while the intensity of UV is influenced by the autoregressive coefficient (β) and the SD of the noise term (σ_θ). We examine the impact of EV on the evolution of cooperation under three scenarios: RV, UV, and combined variability (CV), where both the SoR shifts and the threshold θ fluctuates.

Game

Communication over resources (such as primitive bartering, giving, looting) between agents is represented by simple pairwise games. These games can only be played with an opponent who is connected through a network edge. The probability that agent i selects agent j as its game opponent from its neighbors is $p_{i,j}^G = \frac{1}{n}$; n is the number of neighbors of i, and neighbors refer to agents directly connected to i in the interaction structure network. The game procedure follows a pairwise public goods game (PGG) [64–67] with resource threshold considerations. First, assume that agent i selects agent j. If the agent is C, it contributes a surplus resource $M_i = \max(r_i - \theta, 0)$. If the agent is D, it does not contribute any resource. The contributed resources are multiplied by a factor b ($1 \leq b \leq 2$) and then equally divided between i and j.

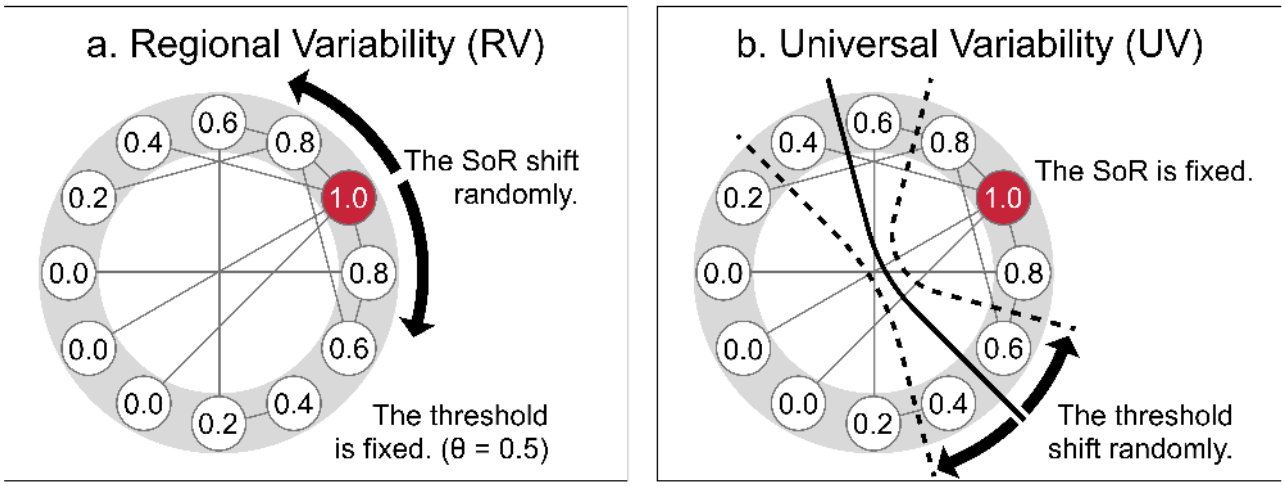

Figure 2.1: Relationships, geographical structure, and EV. Each small circle within the gray circle represents a group (agent, node), with the number inside indicating the resource value. The gray ring represents the geographical structure, and each line connecting agents denotes a relationship (edge). (a) In the RV model, the SoR shifts randomly within the geographical structure, and resources are then allocated to other nodes. Following this, the game and reformation processes occur. The resource threshold for reformation is fixed at $\theta = 0.5$. (b) In the UV model, the SoR remains fixed, but the threshold θ fluctuates randomly, following an AR(1) process.

The payoff table is as follows:

	C	D
C	R_i, R_j	S_i, T_j
D	T_i, S_j	P_i, P_j

(2.1)

$$R_i = \left(\frac{b}{2} - 1\right) M_i + \frac{b}{2} M_j \tag{2.2}$$

$$S_i = \left(\frac{b}{2} - 1\right) M_i \tag{2.3}$$

$$T_i = \frac{b}{2} M_j \tag{2.4}$$

$$P_i = 0 \tag{2.5}$$

The social optimum, which maximizes the sum of both payoffs, is CC under $b > 1$. The Nash equilibrium is DD when $b < 2$. Thus, a social dilemma exists across the defined range of b, except at the boundaries. Additionally, by solving $T_i > R_i > P_i > S_i$, the condition for the game to qualify as a prisoner's dilemma is $b > 1 + \frac{M_i - M_j}{M_i + M_j}$. If this condition is not met, then $T_i > P_i > R_i > S_i$.

We have chosen this game model instead of classic pairwise games to implement the condition that only agents with surplus resources can contribute to other agents. In classic pairwise games, such as the prisoner's dilemma or the snowdrift game, benefits and costs are fixed at

constant values. This implies that agents would cooperate identically, regardless of resource abundance or scarcity, even under uncertain survival conditions. This assumption is inconsistent with our research context. Therefore, we have developed and adopted a novel pairwise PGG model that accounts for resource availability.

Reformation

If, as a result of the games, an agent's resource falls below the threshold θ, it is considered to have failed to adapt to the environment, triggering a reformation of its strategy and network connections. An agent i that falls below θ randomly selects a role model. The probability that j is chosen as its role model is $p_j^R = \frac{r_j}{\sum_{k\in[1,..,N]} r_k}$. Agent i imitates j's strategy, with mutation occurring at a probability μ. Additionally, agents that fall below the threshold disconnect all of their current relationships. They then randomly select the same number of new neighbors as the number of disconnections and establish new connections. The probability that agent j is chosen as a new neighbor is proportional to p_j^R. In other words, the higher the resource, the more likely an agent is to be chosen as a role model and a new neighbor.

Evaluation

The simulation runs for $10,000$ generations, with 100 independent simulations conducted for each parameter set (Table 2.1). Resource allocation and interactions, including games and reformations, occur once per generation. The proportion of agents employing strategy C in each generation is referred to as the cooperation rate. The average cooperation rate is calculated as the mean of the cooperation rates across trials, considering only the last 50% of the generations. To assess the effect of EV on the evolution of cooperation we compared the average cooperation rates across different parameters controlling RV and UV, along with other factors (Table 2.1).

2.2 Results

Effect of RV

We first examined the impact of RV in isolation, without considering UV. Specifically, in each generation, the SoR randomly shifts within the range of $[-\sigma_R, \sigma_R]$, accounting for the periodic boundary condition. The threshold θ, which universally affects the resource welfare of all agents, is fixed at 0.5.

The results (Fig 2.2a) suggest that RV can promote the evolution of cooperation. To elaborate, when the SoR is fixed ($\sigma_R = 0$), cooperation does not evolve. As variability slightly increases ($\sigma_R = 1$), the cooperation rate rises to around 10%. For $b \leq 1.7$, further increases in variability do not promote additional cooperation, although the cooperation rate remains

Table 2.1: Model parameters used in the simulations

Parameter	Description	Value
N	Number of agents	100
n_0^C	Initial number of C agents	0
k_0	Initial degree of the interaction structure network	4
t_{max}	Number of time steps (generations) for a simulation	10,000
$trials$	Number of simulations per parameter set	100
r_{max}	Max resource	1.0
f_{RD}	Resource decrement factor	0.02
σ_R	Shift range of the SoR	$\{0, 1, ..., 49\}$
μ_θ	Expected value of threshold θ	0.5
β	Autoregressive coefficient of the UV	$\{0.0, 0.1, ..., 0.9\}$
σ_θ	SD of the noise term of UV	$\{0.0, 0.1, 0.2\}$
b	Multiplication factor for PGG	$\{1.0, 1.1, ..., 2.0\}$
μ	Mutation rate for strategy imitation	0.01

higher than when $\sigma_R = 0$ or 1. However, for $b \geq 1.8$, greater variability further enhances cooperation.

Despite the overall positive effect of higher variability on cooperation, cooperation is not completely stable and fluctuates with temporary environmental changes. For example, when $b = 1.8$ and $\sigma_R \in [1, 4, 16]$, the temporal transition (Fig 2.2b) shows that the cooperation rate rises and falls dramatically.

Effect of UV

Next, we examined the effects of UV while excluding RV. As previously defined, UV refers to fluctuations in the threshold θ across generations, which uniformly affects all agents. The intensity of this variability is controlled by the autoregressive coefficient β and the SD σ_θ of the noise term in the AR(1) stochastic model. With the SoR fixed at $p = 1$, resources are allocated less as the distance from this node increases.

We found that while UV promotes the evolution of cooperation to some extent, its effect is considerably more limited than that of RV. For $\sigma_\theta = 0.1$, the cooperation rate gradually increases when β exceeds 0.5, but it peaks at just 30% (Fig 2.3a). For $\sigma_\theta = 0.2$, the cooperation rate remains between 20% and 30%, regardless of β, and increasing variability further does not affect these outcomes (Fig 2.3a).

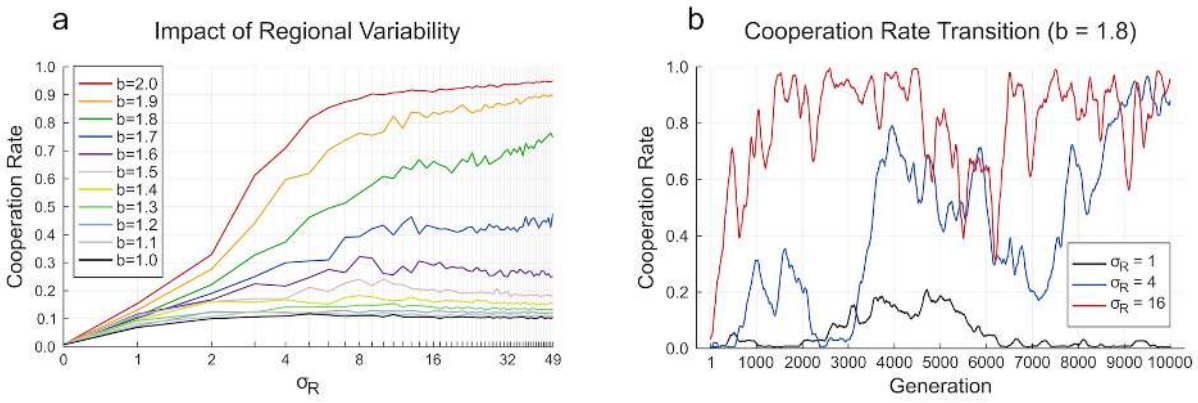

Figure 2.2: The effect of RV. (a) The effect of RV across $b \in [1.0, ..., 2.0]$. The horizontal axis represents the intensity of RV, σ_R, and the vertical axis shows the mean cooperation rate over the last $5,000$ generations, averaged across 100 trials. (b) Examples of cooperation rate transitions when $b = 1.8$ and $\sigma_R \in [1, 4, 16]$. The horizontal axis represents generations, and the vertical axis shows the cooperation rate. Higher RV tends to result in fluctuations of the cooperation rate at higher levels, though convergence is not observed.

Effect of CV

We then examined the combined effects of both RV and UV. The results (Fig 2.4) show that, consistent with the separate analyses above, RV strongly promotes the evolution of cooperation, while UV has much subtle effect.

Primary drivers of the results

The results are driven by two key factors: 1. the effects of mutation and EV, which promote fluctuations in cooperation rates, and 2. the coevolution of cooperation and network structure.

First, RV increases the fluctuations in the cooperation rate, rather than the rate itself. Fig 2.5a shows the effect of EV on strategy distribution in a model that entirely excludes the effects of games and networks. When these effects are excluded, changes in strategy distribution occur solely due to mutation and strategy updating. The Y-axis represents the number of agents generated by mutation in one generation, who then serve as role models for strategy updating in the next generation. These agents are the source of changes in strategy distribution. The line for RV in the figure shows that as the variability increases, the number of mutated role models increases linearly. Fig 2.5b "3. (env, C rate)" shows that the time series of RV and the cooperation rate in each of the 100 trials are completely uncorrelated. Furthermore, the results remain unchanged even when cross-correlation analysis is performed, accounting for time delays. Therefore, it is evident that RV does not directly affect the cooperation rate but instead promote fluctuations in it. This can be explained as follows: agents in poorer regions frequently undergo reformations and mutations. When RV is small, agents rarely accumulate resources in the next generation, causing them to undergo reformations again. However, when variability is

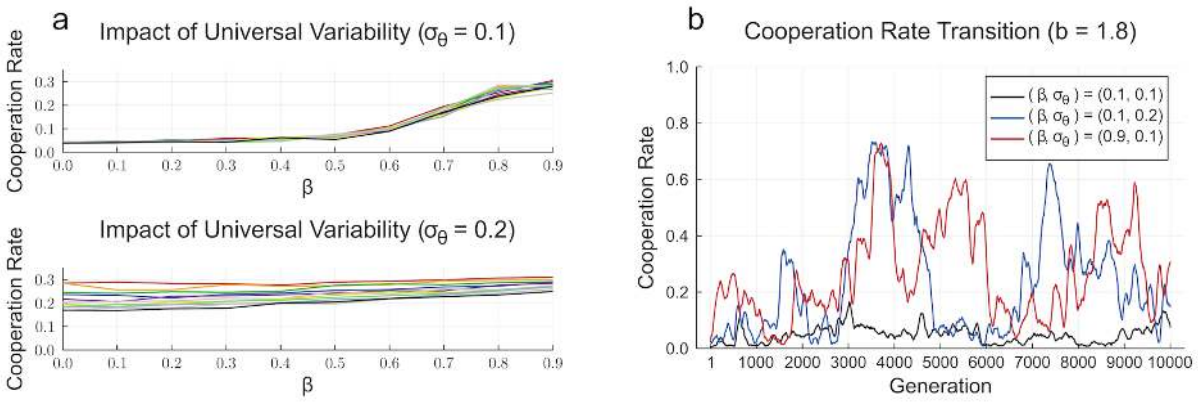

Figure 2.3: The effect of UV. (a) The effect of UV across $b \in [1.0, ..., 2.0]$ and $\sigma_\theta \in [0.1, 0.2]$. The horizontal axis represents the intensity of UV, β, and the vertical axis shows the mean cooperation rate over the last $5,000$ generations across 100 trials. (The line color scheme of these lines is same as in Fig 2.2a.) (b) Examples of the cooperation rate transition when $b = 1.8$ and $(\beta, \sigma_\theta) \in [(0.1, 0.1), (0.1, 0.2), (0.9, 0.1)]$. The horizontal axis represents generations, and the vertical axis shows the cooperation rate. Higher UV tends to result in the cooperation rate fluctuating at higher levels, but convergence is not observed.

large, agents may become resource-rich in the next generation, and they potentially survive to influence the strategy updates of other agents. When RV is large, the cooperation rate is more likely to fluctuate up and down.

Notably, the analytical solution (2.6) aligns closely with the simulation results for RV shown in Fig 2.5a.

$$\begin{aligned} E[n_{MR}] &= \sum_{k=0}^{n} \mu^k (1-\mu)^{n-k} k \frac{\sigma_R}{N} \\ &= \frac{n\mu}{N} \sigma_R \end{aligned} \tag{2.6}$$

In this equation, $E[n_{MR}]$ denotes the expected number of mutated role models, which are generated through mutation and later serve as role models for the strategy updates of other agents. The right-hand side of the equation represents the expected number of mutated agents within a population of reformed agents, n, weighted by the effect of RV, σ_R, across the entire agent population, N. This equation is simplified by applying the formula for the expectation of a binomial distribution.

Second, once the cooperation rate increases, it is likely sustained through the coevolution of cooperation and network structure. Fig 2.5b 7 indicates that the cooperation rate is correlated with the difference in resources between C and D. This correlation likely arises because, as the frequency of C increases, mutual support among Cs strengthens, leading to an increase in the average resources of C. Fig 2.5b 8 further shows that the difference in resources is strongly correlated with the difference in network degree between C and D. This occurs because, in the reformation process of our model, agents with more resources acquire more edges. Finally,

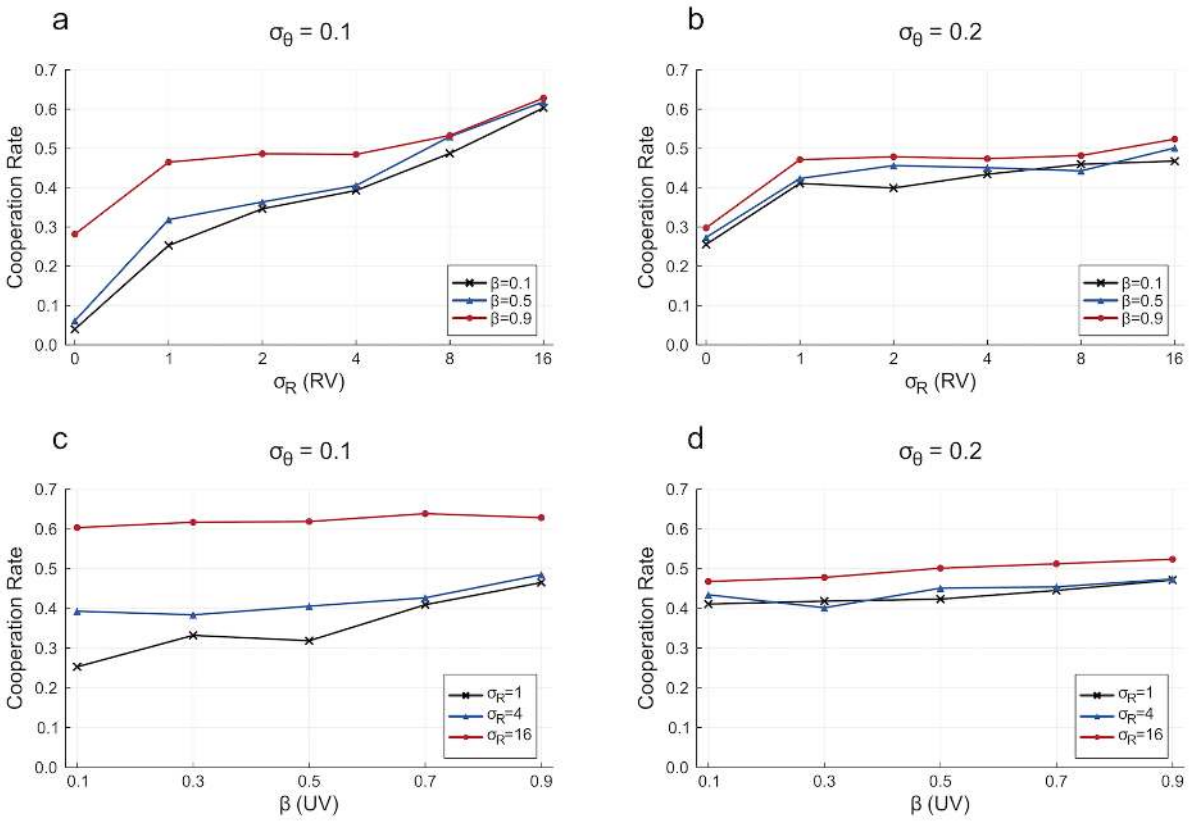

Figure 2.4: The effect of CV ($b = 1.8$). (a) and (b) represent cases with $\sigma_\theta = 0.1$, each with a different x-axis. These plots show that RV increases the cooperation rate significantly, while UV has a limited effect. (c) and (d) represent cases with $\sigma_\theta = 0.2$, with different x-axis. The lines are almost flat except in the range $\sigma_R = 0$ to 1, indicating that when UV is too high, not only UV but even RV has no effect on the cooperation rate.

Fig 2.5b 6 demonstrates that there is a correlation between the difference in degree and the cooperation rate. This is likely because, as shown in several studies [67–69], heterogeneous degree distributions tend to facilitate cooperation in networks. Thus, a positive feedback loop can form, in which an increase in the cooperation rate induces resource heterogeneity, which subsequently results in network degree heterogeneity, and this network heterogeneity, in turn, reinforces the cooperation rate, which is thought to help sustain the maintenance of a cooperation rate that initially emerged by chance. This explanation is based on correlation and inference, and does not rule out the involvement of other factors. One possible factor is the influence of resource heterogeneity on strategy update frequency, which has been suggested to promote cooperation [70]. This process may operate alongside the previously described process where an increase in the cooperation rate widens the resource gap between C and D.

In contrast, UV does not significantly promote cooperation for two reasons: it fails to generate sufficient fluctuation in the cooperation rate, and it inhibits the coevolution of cooperation and the network structure. As shown by the two UV lines in Fig 2.5a, increasing variability does not substantially increase the number of mutated role models, unlike the linear relationship seen with RV. Furthermore, when UV is intense and the threshold θ becomes very large,

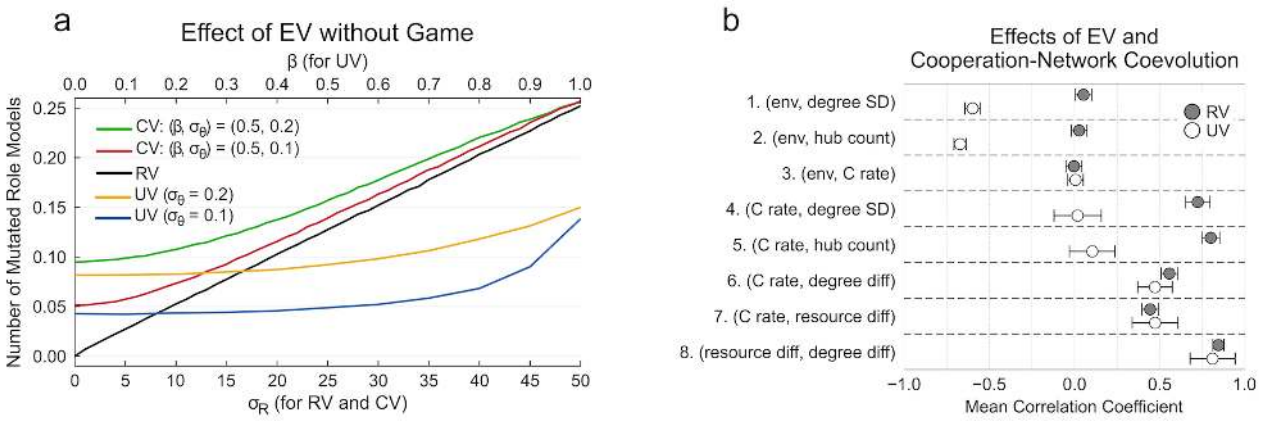

Figure 2.5: Effects of EV on Cooperation. (a) The number of mutated role models as a function of RV and UV. The simulations are based on a model that excludes games. Therefore, the figure shows how EV and reformation impact the system without the effect of games or network structure. (b) Correlation analysis through time series (10,000 generations) between variables related to EV (For RV, env refers to the shift distance of the SoR per generation; for UV, env refers to the value of threshold θ), network structure (degree SD: standard deviation of degrees, hub count: number of nodes with a degree of 10 or more), and cooperation (C rate: frequency of C, resource diff: the difference in average resources between C and D, and degree diff: the difference in average degree between C and D). The mean correlation coefficients are averaged over 100 trials for both RV and UV. $b = 1.8$ for all simulations, $\sigma_R = 16$ for RV, and $\beta = 0.7$, $\sigma_\theta = 0.1$ for UV.

almost all agents undergo reformation. This leads to a reduction in network heterogeneity, which is critical for the coevolution of cooperation and network structure. This is reflected by the strong inverse correlation between UV and network heterogeneity (Fig 2.5b 1-2). The factors that promote cooperation in RV are ineffective in the context of UV, which explains why UV does not significantly promote cooperation. When RV and UV are combined in the CV model, the results remain consistent, RV promotes cooperation, while UV has a much smaller effect.

In summary, the observed patterns in cooperation rates can be attributed to the combined effects of mutation and EV, as well as the coevolution of cooperation and network structure. Specifically, when these two factors work well together, as in the RV model, environmental change promotes cooperation. However, when the first factor is weak and inhibits the second, as in the UV model, cooperation is less likely to evolve.

2.3 Summary

This chapter examined the effects of EV on the evolution of intergroup cooperation using a base model without migration. The results show that RV strongly promotes cooperation, while UV has a weaker effect. These differences arise from two key factors: the fluctuations in strategy distribution generated by EV, and the coevolution of cooperation and network structure. Both

factors work effectively under RV, whereas under UV, neither factor operates effectively due to insufficient fluctuations and disrupted network heterogeneity.

These findings provide a foundation for examining cooperation under EV. The next chapter, Chapter 3, extends this base model by incorporating individual-level migration to examine the combined effects of EV and migration.

Chapter 3

The 2-level model with migration

NOTE: This chapter is based on an ongoing manuscript. The Model section is approximately 80% complete, and the Results section is approximately 50% complete. Both sections will be finalized and integrated into the dissertation structure.

3.1 Model

This model is designed to explore the effects of environmental variability and agent mobility on the evolution of cooperation.

Agent, group and structure

We consider the model composed of multiple regional groups, each inhabited by a number of humans who may migrate between the groups in response to environmental or social pressures. Within this world, the population is represented by agents and regional groups, and their interaction (see Subsection 3.1) and migration (see Subsection 3.1) are governed by the geographical and interaction structures (see Figure 3.1).

In this model, there are n_F agents and n_R regional groups. An agent is an abstract representation of the minimal unit of human migration, such as a family. A group represents the set of agents within a geographically dispersed human habitat.

The geographical structure constrains the positions of groups and the migration of agents. It is defined as a circular graph, i.e., a ring structure, in which each group is connected to its two neighboring groups. These connections remain fixed throughout the simulation. The agents are initially distributed evenly across all groups and can migrate between neighboring groups during the simulation. The migration results in uneven spatial distributions of agents over time, and some groups can be empty.

The interaction structures constrain the selection of opponents for cooperative or competitive interactions at two levels, i.e., inter-group and intra-group (between agents). There is

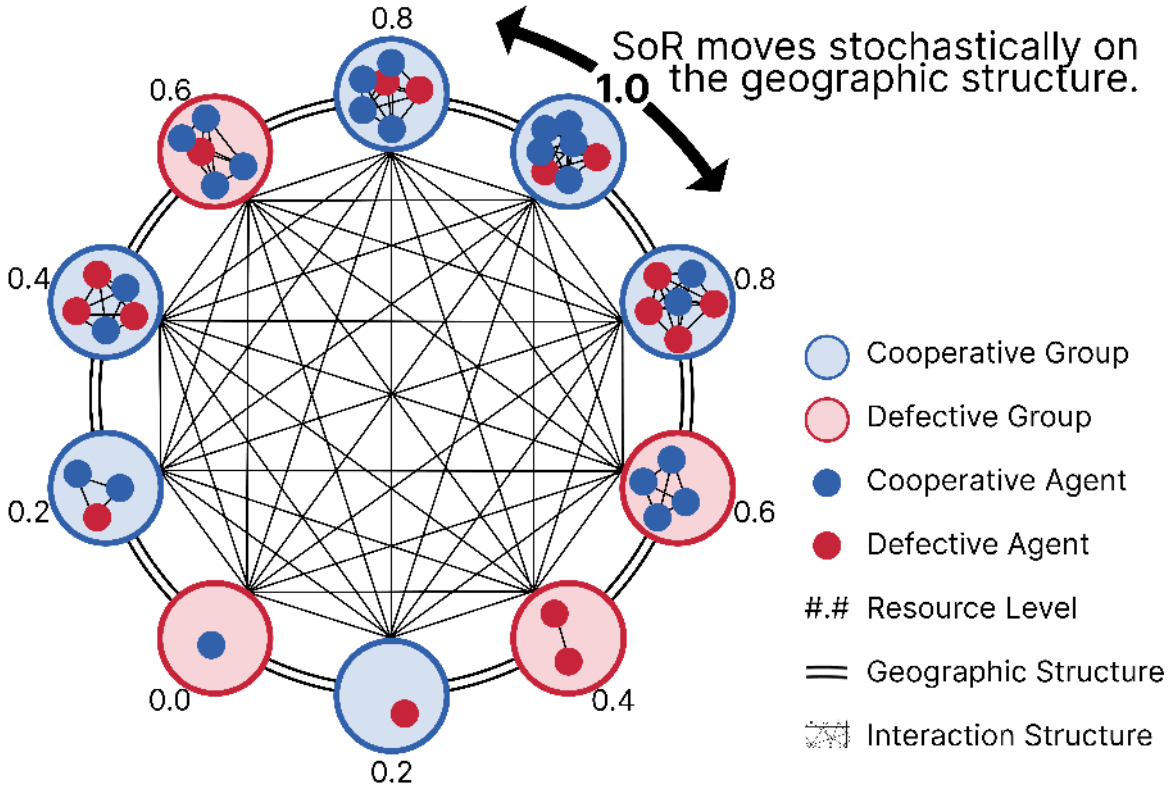

Figure 3.1: Illustration of the model structure. Regional groups are arranged on a circular geographic structure, where the SoR stochastically moves between groups. Each group contains agents. Each group and each agent independently adopt either C (blue) or D (red). Numbers indicate group resource levels, which decrease with distance from the SoR. Interaction structures exist at the group level and at the agent level within each group.

a single inter-group interaction structure in the model, while each group has its own intra-group interaction structure and no interactions occur between agents belonging to different groups. An interaction structure is represented by a weighted, undirected, complete graph whose edge weights are dynamic while its topology remains fixed. The dynamic edge weight $w_{i,j}$ ($0 \leq w_{i,j} \leq 1$, initialized at w_0) denotes the strength of the relationship between nodes i and j, where a node represents either a group or an agent, and is proportional to the probability of interaction between them.

Given these structural foundations, the simulation proceeds in four stages: environmental variability, game, migration, and strategy update. Game and strategy updates occur at both the group and agent levels, in that order. Each stage is described in the following subsections.

Environmental variability

The model captures a key feature of the environmental variability observed during the MSA in Africa, namely the unpredictable shifts in the geographical distribution of resources.

To represent this type of variability, we define the source of resources (SoR) as a dynamic point corresponding to the most resource-abundant region. The SoR moves stochastically across the regional groups introduced in Subsection 3.1 at each simulation time step. This stochastic movement is formalized as

$$x_{t+1} = \begin{cases} [(x_t + \Delta_t - 1) \bmod n_R] + 1, & \text{with probability } p_{EV}, \\ x_t, & \text{otherwise,} \end{cases} \tag{3.1}$$

where x_t denotes the index on the circular graph of regional groups indicating the position of the SoR at time t, $\Delta_t \in \{-1, +1\}$ is chosen with equal probability, and p_{EV} is a key parameter controlling the intensity of the environmental variability.

The group at which the SoR is located receives a resource value of 1. The amount of resources allocated to other groups decreases with their distance from the SoR along the geographical structure, reaching 0 for the group farthest from the SoR. This resource allocation is formalized as

$$r_i^R = 1 - \frac{d_i}{\left\lfloor \frac{n_R}{2} \right\rfloor} \tag{3.2}$$

where r_i^R denotes the resources received by group i, and d_i is the distance between group i and the SoR, calculated with periodic boundary conditions. The resources of each group are evenly shared among its agents.

Game

Interactions that affect gains and losses of resources, both between groups and between agents, are modeled using a game-theoretic framework. Because interactions at the group and agent levels often follow the same rules, we occasionally use the term *entity* as a general label for both. Entity i adopts a strategy $s_i \in \{C, D\}$, where C denotes cooperation and D denotes defection. The interaction dynamics consist of three sequential phases: opponent selection, a pairwise public goods game (PGG), and an update of the interaction structure.

The opponent selection is based on the relationships between entities specified by the edge weights of the interaction structure. Each entity i stochastically selects another entity as its opponent, with the probability of selecting entity j given by

$$P(j|i) = \frac{w_{i,j}}{\sum_{k \neq i} w_{i,k}}. \tag{3.3}$$

Each selected pair then engages in a pairwise PGG. Here, we employ a pairwise PGG rather than traditional pairwise games such as the Prisoner's Dilemma Game and the Stag Hunt Game in order to incorporate both the resource value of each entity and the relationships into the game. In the game between entity i and j, both contribute their respective amounts c_i and c_j; the total contribution is multiplied by a constant factor b, and the amplified resources are then shared equally between them. Specifically, c_i is defined as

$$c_i = \begin{cases} r_i \times w_{i,j}, & \text{if } s_i = C, \\ 0, & \text{if } s_i = D \end{cases} \tag{3.4}$$

where r_i denotes the resource available to entity i at the time of the game. In summary, the payoff matrix for entities i and j is

	C	D
C	$\frac{(c_i+c_j)b}{2} - c_i, \frac{(c_i+c_j)b}{2} - c_j$	$\frac{c_i b}{2} - c_i, \frac{c_j b}{2}$
D	$\frac{c_i b}{2}, \frac{c_j b}{2} - c_j$	$0, 0.$

(3.5)

Finally, the edge weights of the interaction structure are updated to reflect the outcomes of the pairwise games. Because entities benefit from being connected to C but not to D, the direction of change depends on the combination of strategies. When C–C, each has an incentive to strengthen the tie, and the relationship becomes stronger. When C–D or D–C, one side tends to strengthen while the other tends to weaken the tie; these opposing tendencies cancel out, and the relationship remains unchanged. When D–D, each has an incentive to weaken the tie, and the relationship becomes weaker. Formally, the update of the edge weights is given by

$$w'_{i,j} = w_{i,j} + (T - w_{i,j})\Delta w, \tag{3.6}$$

where Δw ($0 \leq \Delta w \leq 1$) denotes the update rate, and the target value T is set to 1 if C–C, $w_{i,j}$ if C–D or D–C, and 0 if D–D.

Migration

Agents facing resource scarcity stochastically migrate to an adjacent regional group in search of better conditions. Specifically, the probability that migration occurs is given by

$$\max\left(1 - \frac{r_i^F}{\theta_F}, 0\right) \cdot p_M, \tag{3.7}$$

where r_i^F denotes the resource available to agent i, θ_R ($0 < \theta_R < 1$) is the universal threshold shared by all groups, θ_F is the per-agent threshold obtained by $\theta_F = \frac{\theta_R}{n_F/n_R}$, and p_M is a parameter controlling the frequency of migration events.

The migration direction is also probabilistic: with probability p_{SoR}, the agent moves to the neighboring group closer to the SoR; otherwise, it chooses randomly between the two neighboring groups.

Upon migration, the agent establishes new relationships in the destination group, and discards all previous ones. Specifically, the edge weights between the agent and the others in the destination group are set to w_0, and the edge weights between the agent and the others in the original group are set to 0.

Strategy update

Entities stochastically update their strategies in response to resource scarcity. Specifically, the probability that an update occurs is given by $\max\left(1 - \frac{r_i}{\theta}, 0\right) \cdot p_{SU}$, where p_{SU} is a parameter controlling the frequency of strategy update events. An entity i that updates its strategy stochastically selects another entity j as its role model, with the probability given by

$$Q(j|i) = \frac{R_j}{\sum_{\substack{k \neq i \\ R_k > \theta}} R_k} \tag{3.8}$$

where θ denotes the relevant threshold, i.e., θ_R at the group level and θ_F at the agent level. The adopted strategy is then subject to mutation with probability μ, resulting in a stochastic switch between C and D. After the update, all edges of the updated entity are reset to the baseline weight w_0.

Evaluation

To examine how environmental variability and agent mobility influence the evolution of cooperation, we conduct simulations across a range of parameter settings, as summarized in Table 3.1. For each setting, 100 independent runs of 10000 generations are carried out. As the principal

performance indicators, we calculate the cooperation rates ϕ_R^C and ϕ_F^C, defined as the average proportions of groups and agents, respectively, employing strategy C during the last 5000 generations and averaged over all runs.

Table 3.1: Model parameters used in the simulations

Parameter	**Description**	**Value options**
n_R	Number of regional groups	$10 \times 2^{\{0,1,2,3\}}$
n_F	Number of agents	$100 \times 2^{\{0,1,2,3,4,5,6\}}$
ϕ_C^0	Initial frequency of cooperators	$\{0, 0.5, 1\}$
w_0	Initial edge weight	$\{0, 0.1, \ldots, 1.0\}$
p_{EV}	Probability factor for environmental variability	$\{0, 0.1, \ldots, 1.0\}$
θ_R	Resource threshold at group level	0.5
b	PGG multiplier	$\{1.0, 1.1, \ldots, 2.0\}$
Δw	Update rate of edge weights	$\{0, 0.1, \ldots, 1.0\}$
p_M	Probability factor for migration events	$\{0, 0.1, \ldots, 1.0\}$
p_{SoR}	Probability of migrating toward SoR	$\{0, 0.1, \ldots, 1.0\}$
p_{SU}	Probability factor for strategy update events	0.1
μ	Mutation probability in strategy update	$\{0, 0.01, 0.05, 0.1\}$

3.2 Results

Influence of environmental variability and agent mobility

We conducted computational experiments to investigate how the environmental variability (p_{EV}) and the agent mobility (p_M) affect the cooperation rates at both the group (ϕ_C^R) and agent levels (ϕ_C^F).

Both ϕ_C^R and ϕ_C^F increase with p_{EV}, though with different patterns. At the group level (Figure 3.2a), ϕ_C^R values are around 0.5 at $p_{EV} = 0$, increase sharply to approximately 0.7 by $p_{EV} = 0.1$, and then increase gradually to approximately 0.8 for $p_{EV} > 0.1$. This pattern does not depend on p_M. At the agent level (Figure 3.2b), ϕ_C^F values are below 0.1 at $p_{EV} = 0$ except at $p_M = 0$; however, they increase steeply by $p_{EV} = 0.1$ and plateau at levels determined by p_M for $p_{EV} > 0.1$.

While p_M does not affect ϕ_C^R (Figure 3.2c), p_M significantly influences ϕ_C^F (Figure 3.2d). When $p_{EV} > 0$, ϕ_C^F is approximately 0.6 at $p_M = 0$, increases to 0.8–0.9 at $p_M = 0.1$, and then decreases linearly for $p_M > 0.1$. In contrast, when $p_{EV} = 0$, ϕ_C^F starts at approximately 0.45 at $p_M = 0$ and declines rapidly as p_M increases.

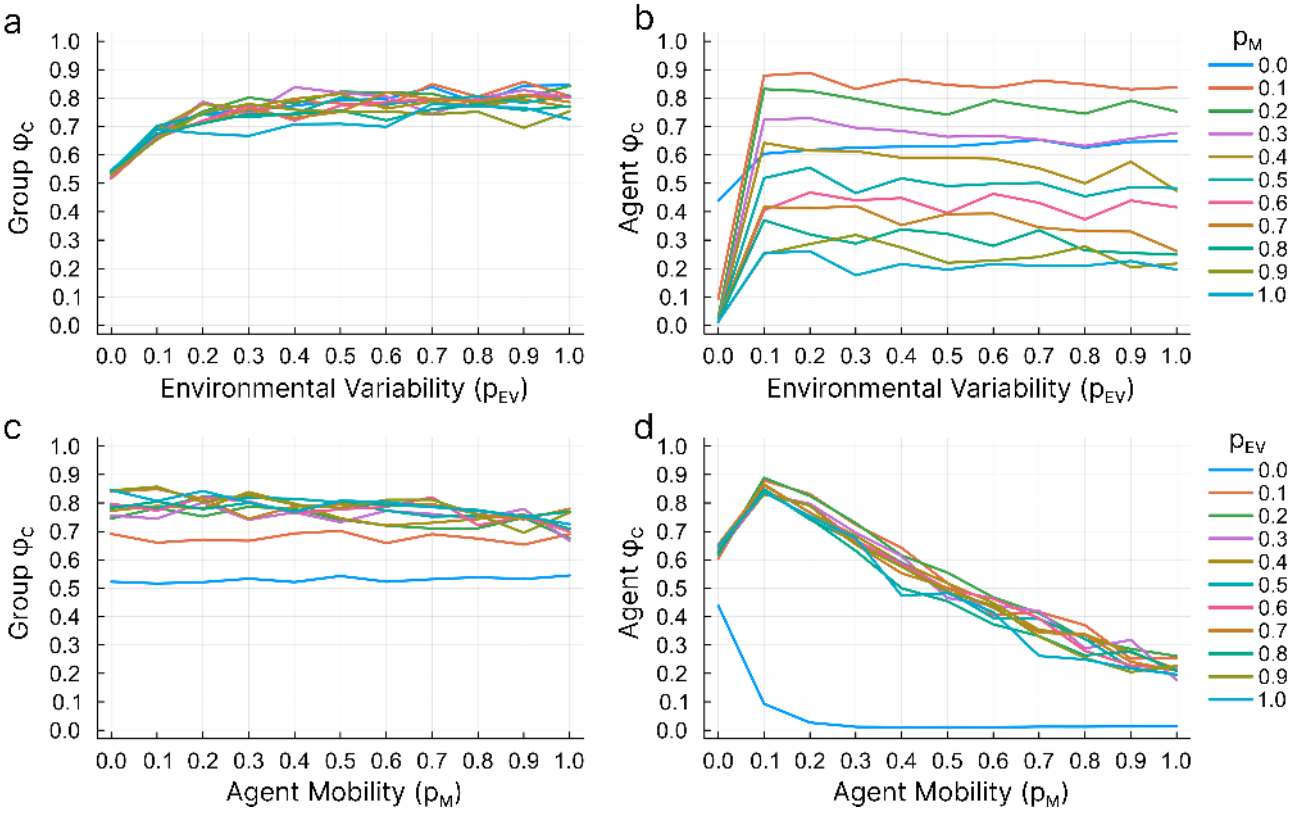

Figure 3.2: Average cooperation rates as functions of p_{EV} and p_M. (a) ϕ_C^R vs. p_{EV} for different p_M values. (b) ϕ_C^F vs. p_{EV} for different p_M values. (c) ϕ_C^R vs. p_M for different p_{EV} values. (d) ϕ_C^F vs. p_M for different p_{EV} values. Each data point represents the mean across 100 independent trials, where each trial is averaged over the final 5000 generations. Other parameters: $n_R = 10$, $n_F = 100$, $\phi_C^0 = 0.5$, $w_0 = 0.3$, $\theta_R = 0.5$, $b = 1.9$, $\Delta w = 0.1$, $p_{SoR} = 0.1$, $\mu = 0.01$.

Figure 3.3 shows standard deviations corresponding to Figure 3.2. Although the mean values exhibit clear patterns (Figure 3.2), the high inter-trial variability arises because ϕ_C^R and ϕ_C^F do not stabilize over time within each individual trial, with different trials converging toward either 0 or 1.

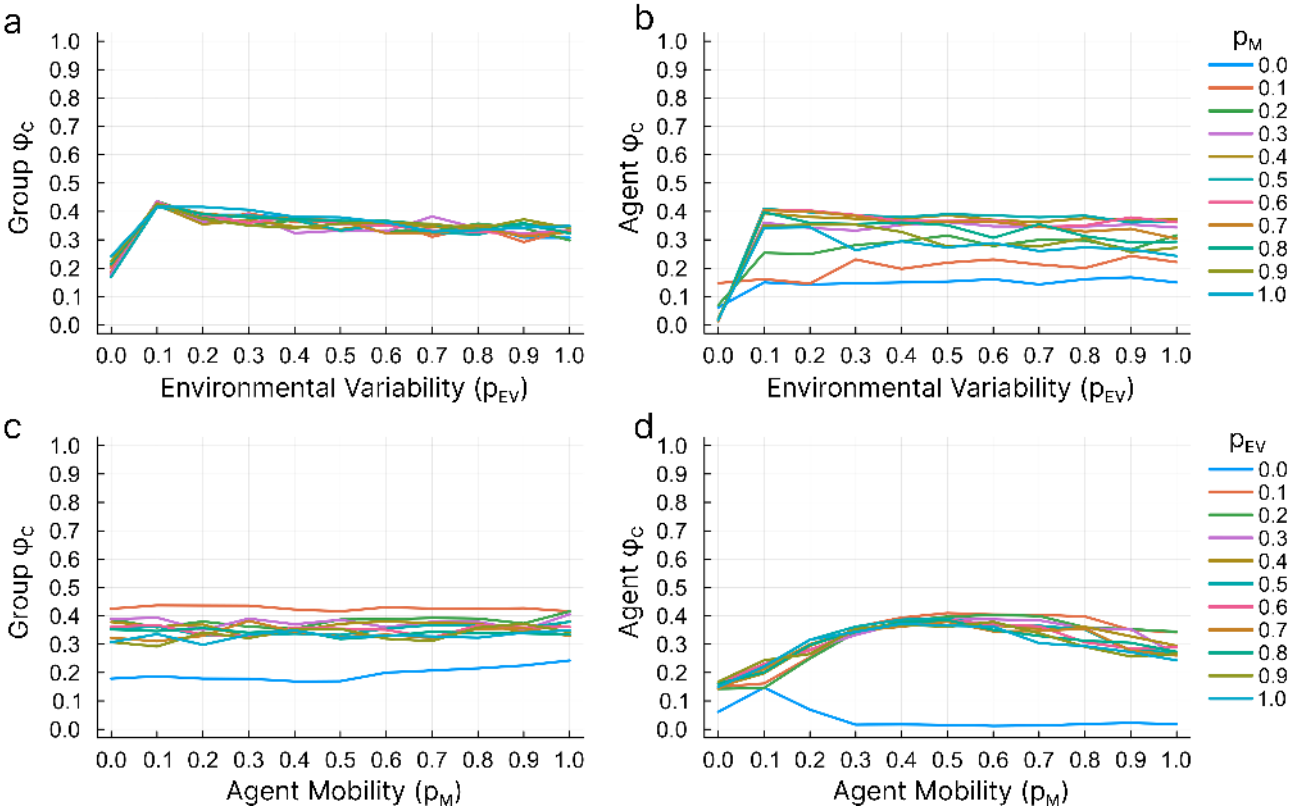

Figure 3.3: Standard deviations corresponding to Figure 3.2.

To examine the direction of influence between the group-level and agent-level processes, we conducted ablation experiments by selectively disabling specific model components. The results show that disabling agent-level games, migration, and strategy updates does not significantly affect ϕ_C^R values (compare Figure 3.2a,c to Figure 3.4a,c), whereas disabling group-level games and strategy updates markedly suppresses ϕ_C^F values (compare Figure 3.2b,d to Figure 3.4b,d). This asymmetry indicates that group-level processes contribute to agent-level cooperation, while the reverse influence is minimal.

The evolution of group-level cooperation by environmental variability can be explained by temporal resource distribution patterns (Figure 3.5). When $p_{EV} = 0$, the resource-rich region remains fixed at group 1, creating persistent spatial inequality where groups near SoR remain resource-rich and maintain stable strategies, while distant groups experience resource scarcity and undergo frequent strategy updates (Figure 3.5a). This spatial segregation prevents the formation of stable cooperative networks across the entire groups. In contrast, when $p_{EV} > 0$, the location of the resource-rich region shifts over time, ensuring that all regions experience both resource-rich and resource-poor periods. This temporal equity increases the long-term value of

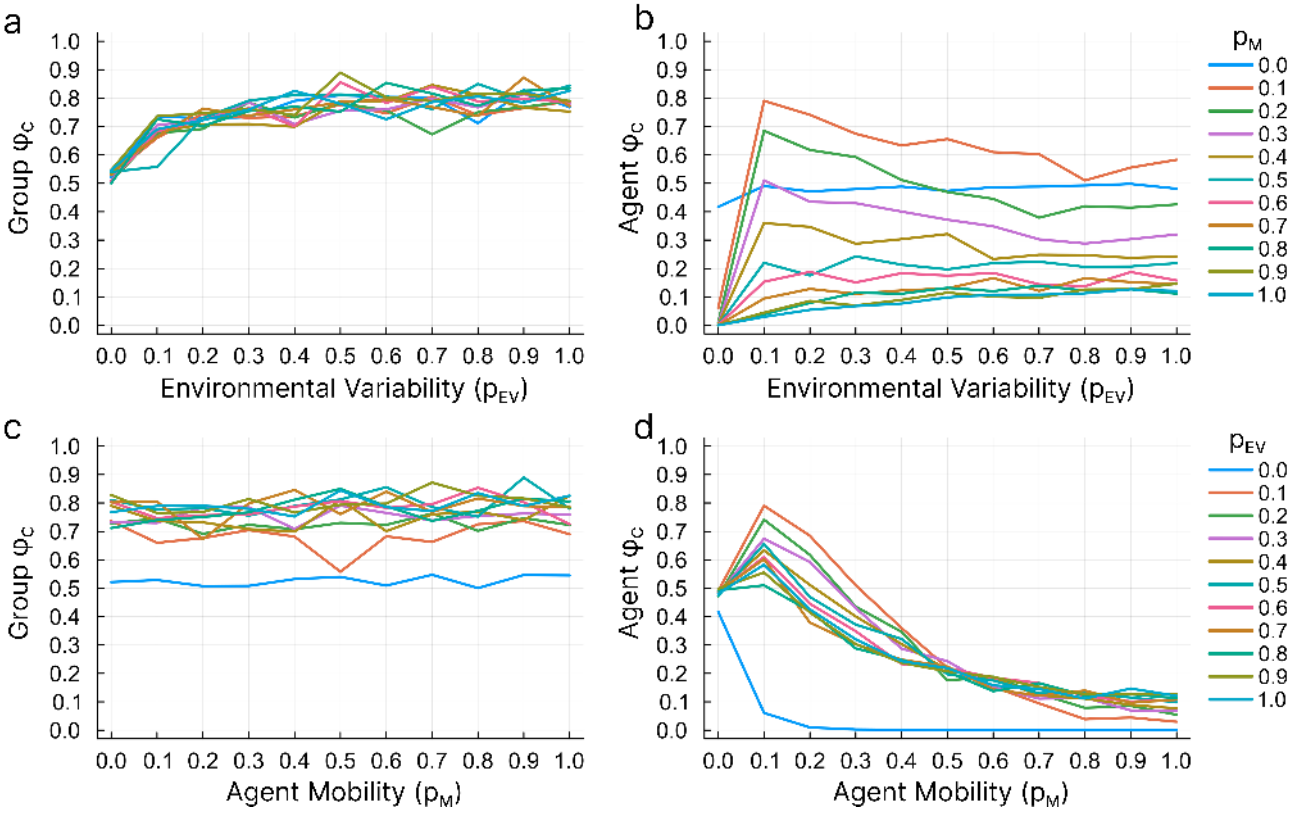

Figure 3.4: Ablation experiments corresponding to Figure 3.2. (a) and (c) show ϕ_C^R when agent level games, migration, and strategy updates are disabled. (b) and (d) show ϕ_C^F when group level games and strategy updates are disabled. Comparison with Figure 3.2 reveals that ϕ_C^R maintains similar patterns regardless of agent level processes, whereas ϕ_C^F is substantially reduced without group level processes. Other conditions are identical to Figure 3.2.

maintaining cooperative relationships through inter-regional games. As shown in Figure 3.5c, cooperative networks gradually form and stabilize throughout the population. Groups adopting C strategies build strong reciprocal relationships, while defecting regions become isolated. These cooperative networks provide resilience against both resource fluctuations and occasional mutations.

ToDo: The evolution of agent-level cooperation by environmental variability can be explained by ...

Influence of population-related parameters

Figure 3.6 shows the effects of population size parameters n_R and n_F on cooperation rates under different environmental and mobility conditions.

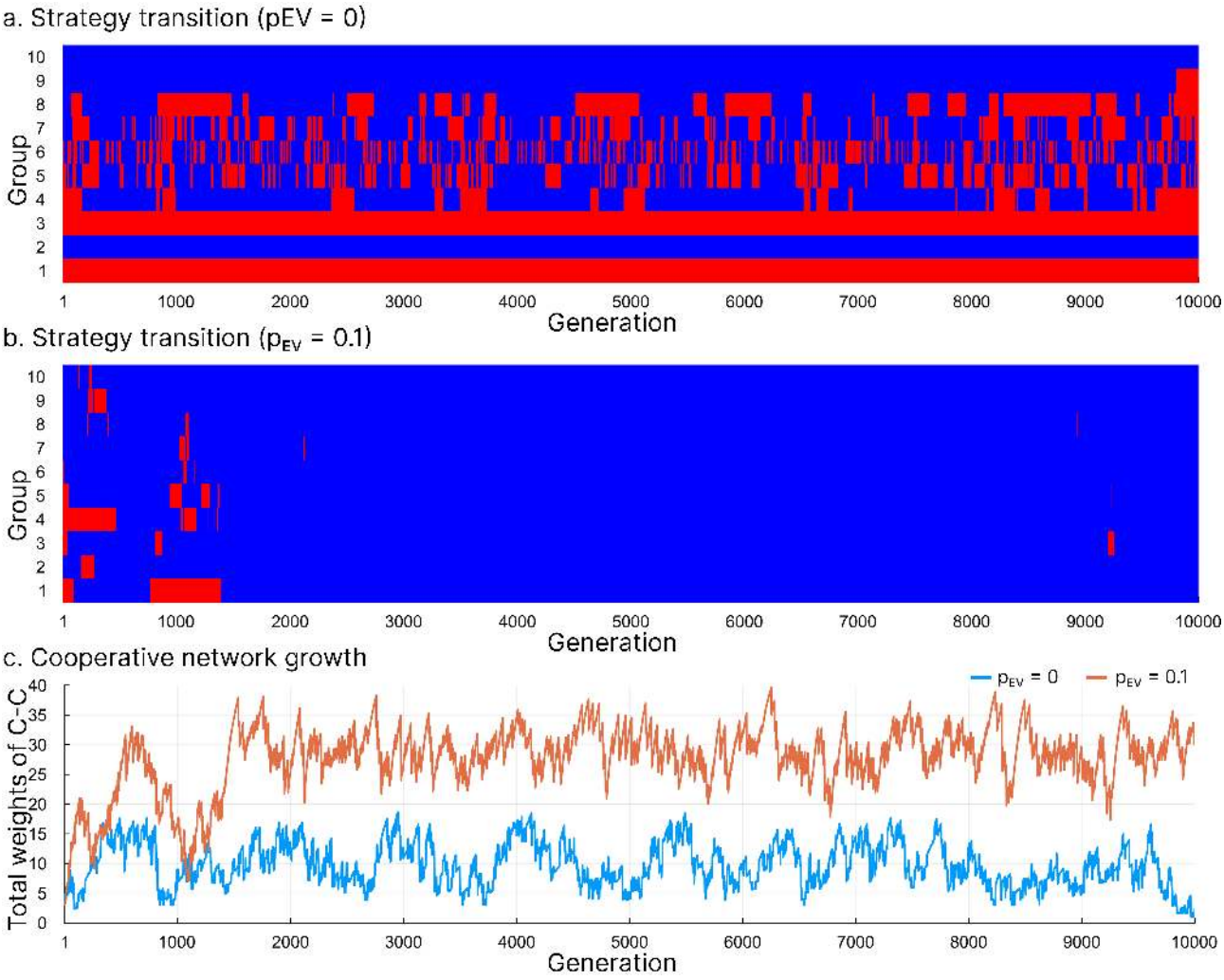

Figure 3.5: Temporal evolution of group-level cooperation. The horizontal axis represents generation, and the vertical axis represents group index. Blue indicates C and red indicates D. (a) shows the case where $p_{EV} = 0$ with the resource-rich region fixed at group 1. (b) shows the case where $p_{EV} = 0.1$ with a shifting resource-rich region. Occasional mutations introduce D, but they quickly revert to C. (c) shows the the transition of the sum of weights between C and C. Other conditions are identical to Figure 3.2.

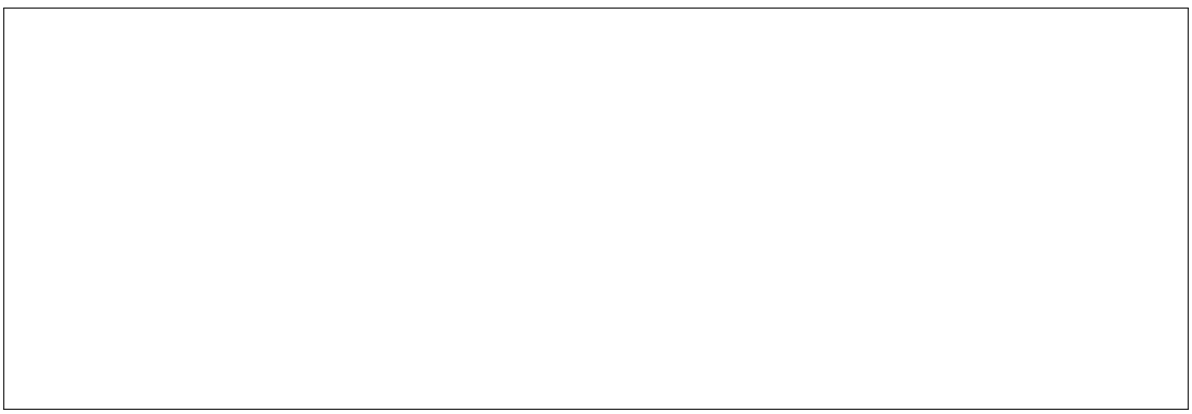

Figure 3.6: Placeholder figure for population size effects (n_R, n_F) under varying p_{EV} and p_M.

When $p_{EV} = 0.0$ and $p_M = 0.0$, both n_R and n_F have negligible effects on ϕ_C^R and ϕ_C^F

(Figure 3.6a,b). When $p_{EV} = 0.0$ and $p_M = 0.1$, ϕ_C^R remains unaffected by population sizes (Figure 3.6c), whereas ϕ_C^F increases with both n_R and n_F (Figure 3.6d).

Under dynamic environmental conditions with $p_{EV} = 0.5$ and $p_M = 0.0$, ϕ_C^R decreases slightly with increasing n_R but remains largely unaffected by n_F (Figure 3.6e). At the agent level, ϕ_C^F decreases slightly with increasing n_R but increases slightly with increasing n_F (Figure 3.6f). These patterns remain essentially unchanged when p_M increases to 0.1 (Figure 3.6g,h).

The initial cooperation rate ϕ_C^0 influences the evolutionary outcomes (Figure 3.7).

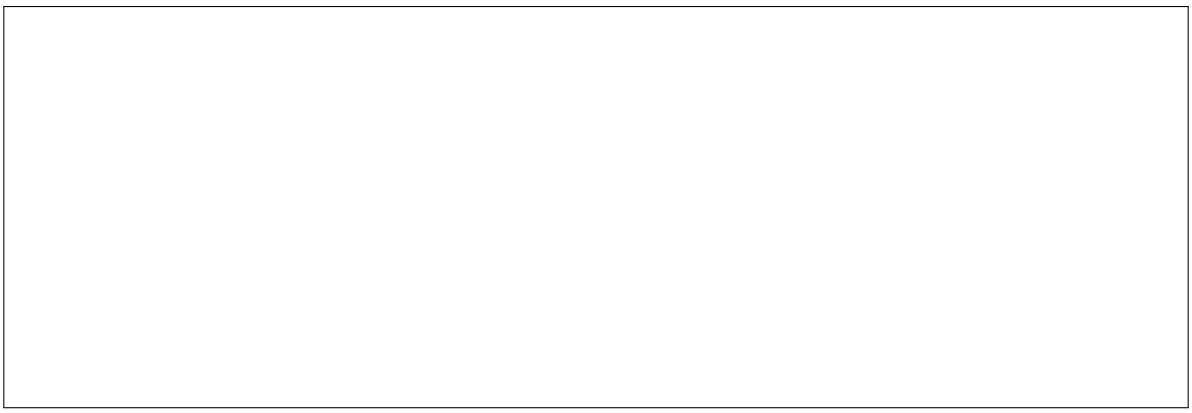

Figure 3.7: Placeholder figure for effects of initial cooperation rate ϕ_C^0.

When $\phi_C^0 = 0$, cooperation rates are lower overall compared to $\phi_C^0 = 0.5$ (Figure 3.2), but the qualitative patterns remain unchanged. In contrast, when $\phi_C^0 = 1$, the patterns change dramatically. Both ϕ_C^R and ϕ_C^F approach 1.0 when $p_{EV} = 0$ and decline as p_{EV} increases. Similarly, both cooperation rates approach 1.0 when p_M ranges from 0 to 0.1 and decline as p_M increases beyond this range.

Influence of network parameters

The initial network weight w_0 influences cooperation evolution at both levels, with smaller values promoting higher cooperation rates (Figure 3.8).

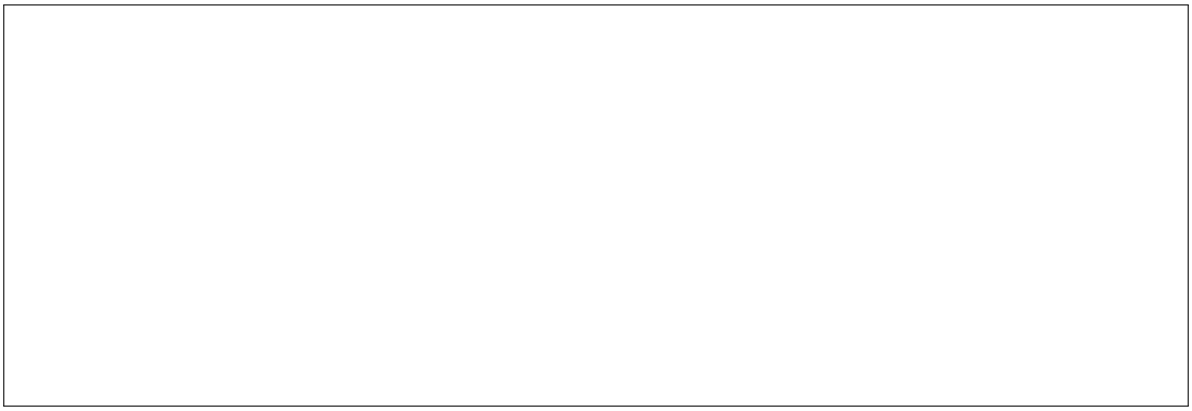

Figure 3.8: Placeholder figure for effects of initial network weight w_0.

This occurs because w_0 determines the interaction strength with newcomers introduced through strategy updates or migration. When w_0 is small, newcomers have weak initial relationships with existing members, limiting their immediate impact on the system. If a newcomer adopts defection, the low w_0 prevents strong interactions that could disrupt established cooperative networks. In contrast, when w_0 is large, defecting newcomers immediately engage in strong interactions with cooperative members, potentially destabilizing the cooperative network and reducing overall cooperation rates.

The relation weight update rate Δw positively affects cooperation, with higher values promoting cooperation at both levels (Figure 3.9).

Figure 3.9: Placeholder figure for effects of relation weight update rate Δw.

Higher Δw values enable relation weights between C pairs to rapidly increase and those between D pairs to quickly decline, thereby accelerating the differentiation between C and D relationships. This rapid differentiation amplifies the benefits of cooperation and the costs of defection, strengthening selection pressures that favor cooperative strategies. However, cooperation rates saturate at approximately $\Delta w = 0.3$ as they approach their maximum possible values, beyond which further increases in Δw have minimal additional effects.

Influence of other parameters

We examined the effects of several additional parameters: the SoR orientation (p_{SoR}), the PGG multiplier (b), and the mutation rate (μ). The parameter p_{SoR} has no significant effect on cooperation rates. Higher values of b promote cooperation at both levels, as expected from standard public goods game theory. Higher μ values blur the patterns observed in mean cooperation rates while reducing inter-trial variability, but do not alter the qualitative patterns. Since these results are either trivial or follow directly from model assumptions, detailed results are provided in the Appendix.

3.3 Summary

Chapter 4

The 2-dimensional model with migration

In Chapters 2 and 3, we examined the evolution of cooperation under environmental variability (EV) using models with explicit group structures. Chapter 2 demonstrated that EV can promote cooperation through the interplay between environmental disruptions and social network structures that support cooperation. However, that model does not incorporate mobility, which is an essential trait of pre-sedentary human populations in the Middle Stone Age (MSA). Chapter 3 introduced individual-level migration, but its relatively unique framework limits direct comparison with existing studies on cooperation and migration. In this chapter[1] we adopt a 2-dimensional (2D) spatial structure, which is widely used in the literature, to examine how EV and agent mobility jointly affect the evolution of cooperation.

The evolution of cooperation among mobile agents has been studied actively. Dugatkin and Wilson (1991) [72] performed pioneering work in this area, and Vainstein et al. (2007) [73] subsequently established that mobility promotes cooperation under minimal assumptions. More recently, various migration strategies [74–80] differing in trigger conditions and migration distance have been proposed. However, to the best of our knowledge, no study has examined exogenous EV in the evolution of cooperation with migration.

This chapter addresses this gap by modeling EV as randomly moving resource-rich spots across a 2D space and agent mobility as resource-seeking migration. Through extensive simulations, we examine whether and how these factors jointly promote cooperation.

4.1 Model

In this chapter, we developed a multiagent simulation model to examine how agent mobility and environmental variability jointly influence the evolution of cooperation in spatially structured populations. Due to the limited availability of archaeological data on spatial resource

[1] This chapter is based on Inaba and Akiyama (2025) [71], published in *Chaos, solitons & fractals*.

distributions and hominin behavioral patterns during the MSA, we adopted an abstracted approach that prioritizes the identification of fundamental mechanisms over reproducing specific historical scenarios. This model incorporates four key processes, i.e., (i) environmental variability on a 2D lattice, (ii) pairwise game interactions, (iii) conditional agent migration driven by resource availability, and (iv) strategy updating. These processes are described in the following subsections.

Environmental variability

The spatial structure is represented by a 2D lattice with periodic boundary conditions. Here, N agents are distributed randomly across the cells, and each cell contains at most one agent. Each cell maintains a resource level that varies both spatially and temporally. We define a Source of Resources (SoR) as a focal point that generates spatial resource gradients in the environment, and these SoRs serve as simplified representations of the natural foraging areas commonly found near rivers, lakes, and coastlines. Each SoR creates a gradient where resource availability typically decreases with increasing distance from the SoR. In addition, multiple SoRs may coexist, thereby forming overlapping zones of resource abundance.

In this model, each agent accumulates resources (represented by the agent's fitness value) through interactions, and local prosperity is defined by a resource threshold $\theta_{x,y}$ for each cell (x, y), where $0 \leq \theta_{x,y} \leq 1$. Agents with fitness values that are less than the threshold $\theta_{x,y}$ are more likely to migrate and update their strategies, and agents with fitness values greater than the threshold remain unchanged. Therefore, locations with lower thresholds impose less pressure for behavioral change, indicating that these locations are prosperous and rich in resources. Here, the threshold $\theta_{x,y}$ is determined by the cumulative influence of all SoRs and is calculated as follows:

$$\theta_{x,y} = \frac{D_{x,y} - D_{\min}}{D_{\max} - D_{\min}}, \quad D_{x,y} = \sum_{i=1}^{n_{SoR}} d_{x,y}^{(i)} \tag{4.1}$$

where n_{SoR} denotes the number of SoRs, $d_{x,y}^{(i)}$ denotes the Euclidean distance from cell (x, y) to the i-th SoR, calculated under periodic boundary conditions, and $D_{\min}$ and $D_{\max}$ denote the minimum and maximum values of $D_{x,y}$ across the entire grid, respectively.

We examine two spatial configurations, which we refer to as 1-SoR and 2-SoR. In the 1-SoR configuration (a 200×200 grid), a single SoR generates a concentric resource gradient, capturing the essential geographical pattern of an oasis-like environment (Figure 4.1a). In the 2-SoR configuration (a 400×200 grid), two SoRs generate a corridor of resource gradient, capturing the essential geographical pattern of riverine or coastal environments where resources are distributed along a line (Figure 4.1b).

Environmental variability is modeled through the stochastic movement of SoRs, reflecting the unpredictable nature of the landscape dynamics observed during the MSA in Africa. Each SoR moves to a randomly selected adjacent cell within the Moore neighborhood with a proba-

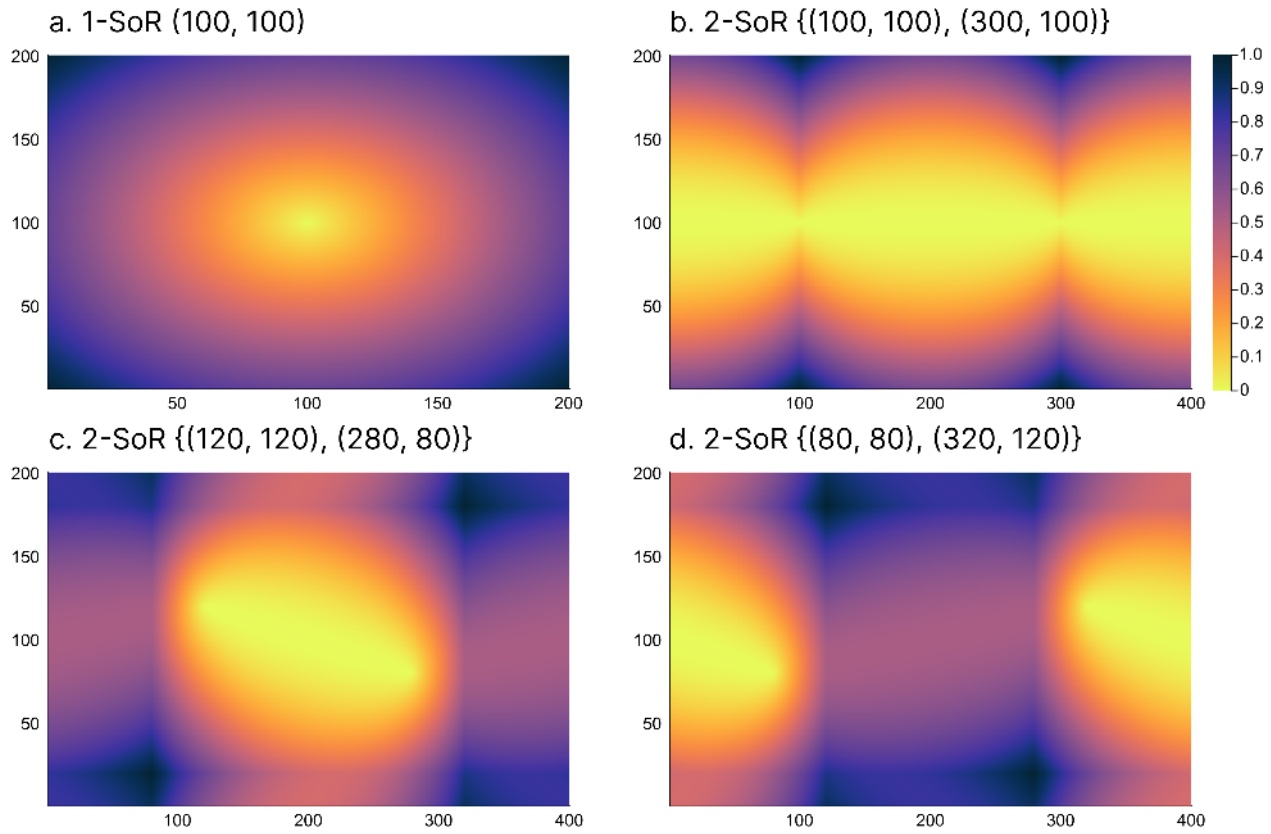

Figure 4.1: Spatially heterogeneous prosperity patterns generated by SoR(s). The colors indicate the resource threshold $\theta_{x,y}$. (a) A single SoR located at $(100, 100)$ on a 200×200 grid generates a concentric resource gradient. (b) Two SoRs located at $(100, 100)$ and $(300, 100)$ on a 400×200 grid generate a band-shaped resource gradient. (c) and (d) Examples of the stochastic movement of SoRs that dynamically reshapes the resource landscapes.

bility p_{EV} $(0 \leq p_{EV} \leq 1)$ at each time step, and the direction is selected uniformly at random from the eight neighboring cells. In this process, the parameter p_{EV} governs the intensity of the environmental variability, where $p_{EV} = 0$ corresponds to a static environment, and higher p_{EV} values represent more intense environmental variability.

Throughout this chapter, the neighborhood is defined as the Moore neighborhood (i.e., eight neighboring cells). This choice better approximates the continuous spatial movement of SoRs and mobile agents than the von Neumann neighborhood (i.e., four orthogonal cells), where movement is restricted to only cardinal directions. In addition, for distance calculations, particularly when determining resource gradients from SoRs, the Euclidean distance is employed to produce smooth, circular gradients that better represent natural resource distributions than other metrics, e.g., the Manhattan or Chebyshev distances.

Game

Games represent cooperative or competitive interactions between agents that involve the gain or loss of resources. Each agent holds a strategy, either cooperation (C) or defection (D),

which determines its behavior in interactions. In every time step, each agent plays pairwise games with all its neighbors and accumulates a payoff π_j, which is then converted into fitness ω_j ($j \in [1, \ldots, N]$, $0 < \omega_j < 1$), representing the agent's resource level.

The payoff matrix of the game is defined as follows:

$$\begin{array}{c|cc} & C & D \\ \hline C & R & S \\ D & T & P \end{array} \tag{4.2}$$

where $R = 1$, $0 < T < 2$, $-1 < S < 1$, and $P = 0$. To ensure the robustness of the results across a range of social dilemma contexts, we consider various game structures, including the Prisoner's Dilemma ($T > R > P > S$), Stag Hunt ($R > T > P > S$), and Snowdrift ($T > R > S > P$) games.

The accumulated payoff π_j is transformed into the fitness ω_j using a sigmoid function as follows:

$$\omega_j = \frac{1}{1 + \exp(-k(\pi_j - \pi_0))} \tag{4.3}$$

where k determines the steepness of the sigmoid curve, and π_0 sets the baseline payoff at which $\omega_j = 0.5$. Here, we set $k = 1$ for moderate sensitivity and set $\pi_0 = 4.0$ to center the sigmoid around common payoff values found in mixed-strategy populations. Given that each agent can accumulate payoffs from up to eight of its neighbors, the theoretical payoff range is $8S$ to $8R$ and $8P$ to $8T$ for cooperators and defectors, respectively. With our parameter constraints, this yields a payoff range of $-8 < \pi_j < 16$.

Migration

At each time step, agents migrate if their fitness ω_j is less than the resource threshold $\theta_{x,y}$ at their current location. Any agent that meets this condition migrates with probability p_M and remains at the location with the complementary probability $1 - p_M$. The migration direction follows a resource-oriented bias, where an agent moves toward a neighboring cell with the lowest $\theta_{x,y}$ value with probability p_{SoR} (SoR orientation) and moves randomly within the neighborhood with the complementary probability $1 - p_{SoR}$. Cells occupied by other agents are excluded from the candidate destinations. The agents migrate asynchronously in a randomized order to avoid movement conflicts.

Strategy update

At each time step, agents update their strategies synchronously if their fitness ω_j is less than the resource threshold $\theta_{x,y}$. Any agent that meets this condition adopts the strategy of the most successful neighbor (i.e., the neighbor with the highest fitness). This process is subject to

mutation, where the adopted strategy is replaced by the opposite strategy (e.g., from C to D or vice versa) with probability μ.

We note that asynchronous updating [81, 82] is more realistic and the choice of updating protocol can significantly affect outcomes in densely packed models [81]. However, unlike densely connected lattice models where agents interact with many neighbors simultaneously, our agents typically interact with only a few neighbors on each resource patch. This sparsity reduces the interdependence between neighboring strategy updates, making the dynamics largely insensitive to the updating protocol.

Evaluation

To investigate the effects of environmental variability and agent mobility on the evolution of cooperation, simulations are performed under a range of parameter configurations, as shown in Table 4.1.

Each configuration is evaluated through 100 independent trials of 10000 generations each. As the primary outcome measure, we compute the cooperation rate ϕ_C, which is defined as the average proportion of agents employing the C strategy during the final 5000 generations averaged over all trials.

Table 4.1: Model parameters used in the simulations.

Parameter	Description	Value options
$W \times H$	Grid dimensions	$200 \times 200, 400 \times 200$
N	Total number of agents	$500 \times 2^{\{0,1,2,3,4,5\}}$
ϕ_C^0	Initial frequency of cooperators	$0, 0.5, 1$
n_{SoR}	Total number of SoRs	1, 2
p_{EV}	Probability of SoR shift	0 to 1 (step: 0.1)
R	Payoff for mutual cooperation	1
T	Payoff for defection against cooperator	0 to 2 (step: 0.1)
P	Payoff for mutual defection	0
S	Payoff for cooperation against defector	-1 to 1 (step: 0.1)
p_M	Probability of migration	0 to 1 (step: 0.1)
p_{SoR}	Probability of resource-oriented migration	0 to 1 (step: 0.1)
μ	Probability of mutation	$0, 0.01$

4.2 Results

Influence of environmental variability and agent mobility

Figure 4.2 shows the combined effects of environmental variability (p_{EV}) and agent mobility (p_M) on the cooperation rate ϕ_C. As can be seen, in stable environments ($p_{EV} = 0$) or with low agent mobility ($p_M \lesssim 0.2$), cooperation fails to evolve. In contrast, with sufficient agent

mobility ($p_M \gtrsim 0.2$), even modest environmental variability ($p_{EV} = 0.1$) promotes cooperation; however, further variability ($p_{EV} > 0.1$) does not enhance cooperation. In addition, agent mobility promotes cooperation with any level of environmental variability ($p_{EV} > 0$).

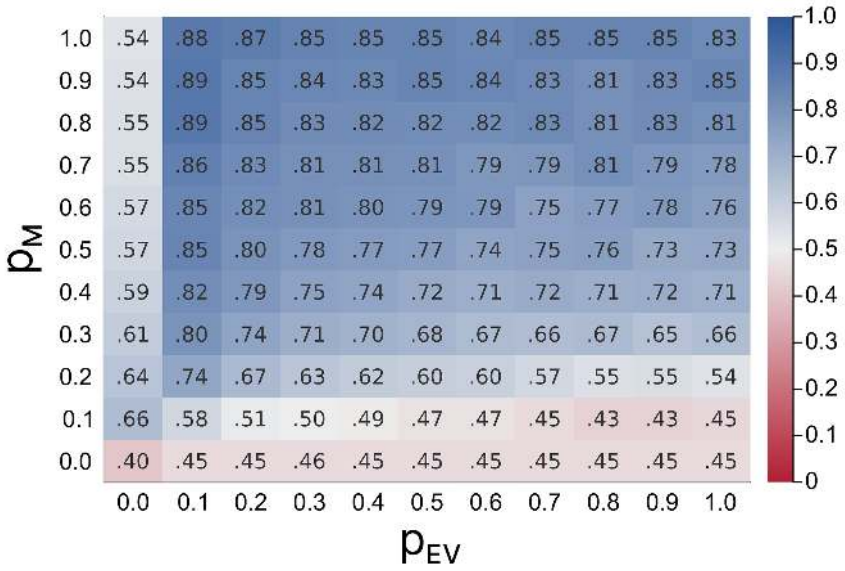

Figure 4.2: Influence of environmental variability (p_{EV}) and agent mobility (p_M) on the cooperation rate (ϕ_C). The figure shows that cooperation emerges only when both $p_{EV} \gtrsim 0.1$ and $p_M \gtrsim 0.2$, with neither factor alone being sufficient to promote cooperation. Each cell shows the mean value over 100 independent runs. The results are shown for a representative parameter set ($N = 1000$, $\phi_C^0 = 0.0$, 2-SoR, $T = 1.2$, $S = -0.2$, $p_{SoR} = 0.1$, $\mu = 0.01$). Qualitatively similar patterns are observed for other parameter configurations. The standard deviations across runs are less than 0.15 for all cells.

Figure 4.3 shows the role of environmental variability in the evolution of cooperation. This representative simulation is presented to understand the temporal dynamics underlying the statistical patterns displayed in Figure 4.2. Whereas Figure 4.2 considers fixed variability levels throughout the simulation, here we apply a cyclic p_{EV} alternating between stable and variable conditions every 2000 generations over a total of 10000 generations. Under these cyclic conditions, cooperation initially increases to slightly less than 50% during the first stable phase and then plateaus, as shown in Figure 4.3a. A pronounced increase is observed once the system enters the variable phase, which reinforces the conclusion that environmental variability plays a pivotal role in promoting cooperation.

The observed dynamics can be understood as a three-stage process: (i) the formation of a few large defector groups fixed in resource-rich areas, (ii) their collapse induced by environmental variability, and (iii) subsequent emergence of several small cooperator groups. Figures 4.3b–f show snapshots from the simulation presented in Figure 4.3a. A full video showing this process is provided in the Appendix. In the first stable phase as shown in Figure 4.3b, the agents in prosperous areas have no need to cooperate or move, whereas those in less prosperous areas must cooperate or move to prosperous areas. At the boundaries between these two areas, fixed

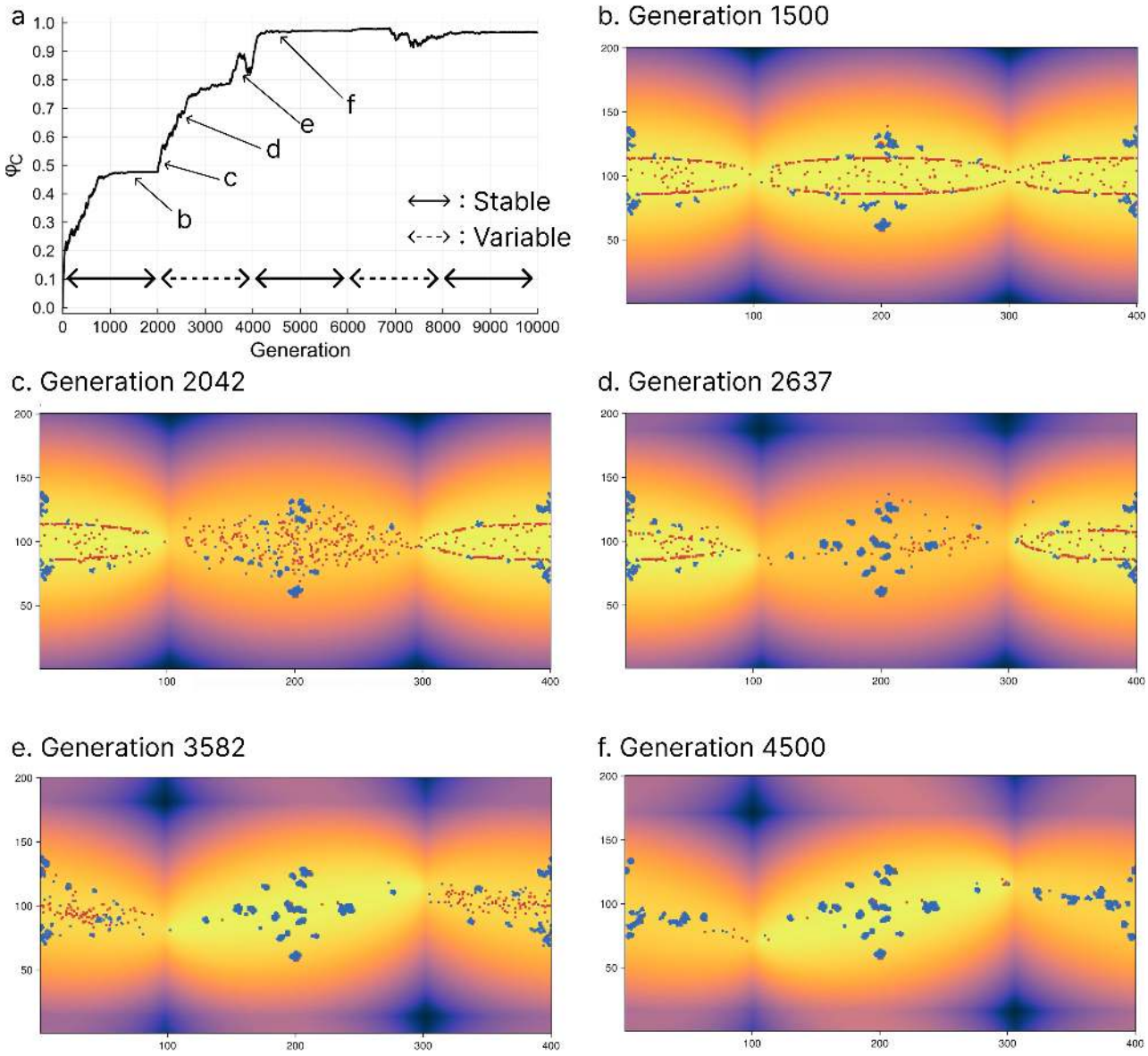

Figure 4.3: Temporal dynamics under cyclic environmental variability. The figure demonstrates that environmental variability drives cooperation by disrupting stable defector groups in resource-rich areas and facilitating the formation of multiple small cooperator groups. (a) Cooperation rate over 10000 generations with p_{EV} alternating between stable ($p_{EV} = 0$) and variable ($p_{EV} = 0.1$) phases every 2000 generations. (b)–(f) Spatial snapshots at each generation. Blue and red dots represent cooperators and defectors, respectively. Background colors indicate the resource threshold $\theta_{x,y}$ as in Figure 4.1. Parameter settings: $N = 1000$, $\phi_C^0 = 0.0$, 2-SoR, $T = 1.2$, $S = -0.2$, $p_M = 1.0$, $p_{SoR} = 0.1$, $\mu = 0.01$.

walls are formed by defectors who do not need to change their strategies or move further. During the next variable phase as shown in Figures 4.3c–e, agents located on boundaries are forced to cooperate or move due to the environmental changes, thereby leading to the collapse of the stable defector group as shown in the central area of Figure 4.3c. In place of the defector group, the agents form several small cooperator groups to survive even in severe environmental conditions (Figure 4.3d). Then, the same process occurs in the areas at both ends of the figure

(Figures 4.3e and f).

In contrast, cooperation cannot evolve if the agent mobility is insufficient relative to the intensity of the environmental variability (refer to the lower area of Figure 4.2), which occurs because excessively rapid SoR movement prevents the formation of both defector structures and small cooperator groups, as shown in Figure 4.4. Thus, environmental variability and sufficient agent mobility promote cooperation by preventing fixed defector structures and encouraging the agents to form cooperator groups for survival.

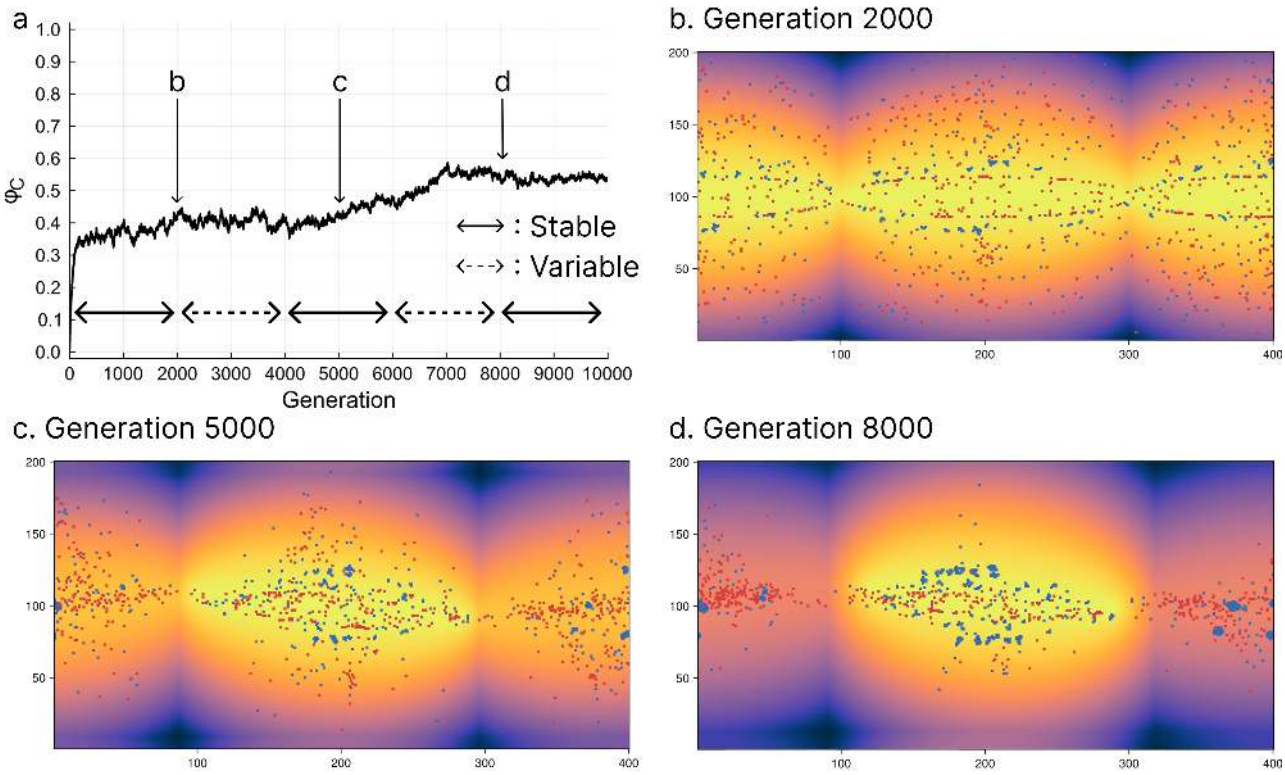

Figure 4.4: Temporal dynamics under cyclic environmental variability with low agent mobility. In contrast to Figure 4.3 ($p_M = 1.0$), here lower mobility ($p_M = 0.1$) prevents agents from keeping up with the environmental variability. As a result, cooperation fails to evolve. All other parameters and the interpretation of the visual elements are the same as in Figure 4.3.

Influence of other parameters on cooperation rate

To gain further insights into the findings presented above and assess their robustness, we investigated the effects of additional parameters, including the population size (N), the number of SoRs (n_{SoR}), the initial frequency of cooperators (ϕ_C^0), the SoR orientation (p_{SoR}), the payoff parameters (T, S), and the mutation rate (μ).

Population size

Larger population size promotes cooperation to some extent, as shown in Figure 4.5, because the cooperators can more easily find other cooperators when the population size is sufficiently

large.

Another notable observation is that the cooperation rates for $(p_{EV}, p_M) = (0.0, 0.1)$ (red dashed line) and $(0.1, 0.1)$ (blue dashed line) exhibit a crossover at approximately $N = 2000$. For small populations ($N < 2000$) with low agent mobility, cooperation evolves more readily without environmental variability. In stable environments ($(p_{EV}, p_M) = (0.0, 0.1)$), both the defector and cooperator groups persist once established, although the formation of these groups is slow due to the low agent mobility. In contrast, environmental variability with low agent mobility ($(p_{EV}, p_M) = (0.1, 0.1)$) creates perpetual fluidity that prevents the formation of both structures.

Larger populations alter this relationship. Larger populations increase the encounter rate among cooperators, which allows for the formation of cooperator groups even under environmental variability. In stable environments, the structures remain fixed, thereby limiting the impact of the higher encounter rate. In contrast, the higher encounter rate in fluid environments facilitates group formation. Thus, environmental variability becomes advantageous for cooperation above the critical population size.

A less prominent but similar crossover occurs at approximately $N = 8000$ between $(p_{EV}, p_M) = (0.0, 0.1)$ (red dashed line) and $(p_{EV}, p_M) = (0.0, 1.0)$ (red solid line). This crossover reflects the spatial constraints of the defector groups in stable environments ($p_{EV} = 0$). For $N \lesssim 8000$, high mobility ($p_M = 1.0$) allows more agents to reach the resource-rich areas where cooperation is not required. In contrast, low mobility ($p_M = 0.1$) keeps the agents in peripheral areas where cooperation is required for survival.

However, larger populations ($N \gtrsim 8000$) exhibit three nested zones: central rich areas, where cooperation is not required; surrounding moderate areas, where the agents can survive through cooperation; and the most peripheral harsh areas, where agents cannot survive even with cooperation because the resource threshold exceeds what can be provided through cooperation. Under these conditions, high mobility allows the agents to escape from the harsh areas to the moderate cooperative areas, whereas low mobility traps the agents in the harsh areas. In addition, the central rich areas have already reached their physical capacity due to the large population; thus, further population increases have no effect in these areas. Consequently, the effect of mobility on the cooperation rate (ϕ_C) reverses as the population size increases.

Number of SoRs and initial cooperator rate

Both the number of SoRs (n_{SoR}) and the initial frequency of cooperators (ϕ_C^0) have a significant influence on the results. While the 2-SoR configuration forms large band-shaped defector groups (Figure 4.3b), the 1-SoR configuration only forms a small, circular resource-rich area (Figure 4.6b). When a large defector group collapses and is replaced by small cooperator groups, as observed with the 2-SoR setting, the impact on the overall system is substantial. In contrast, under the 1-SoR setting, when a small defector group undergoes the same replacement,

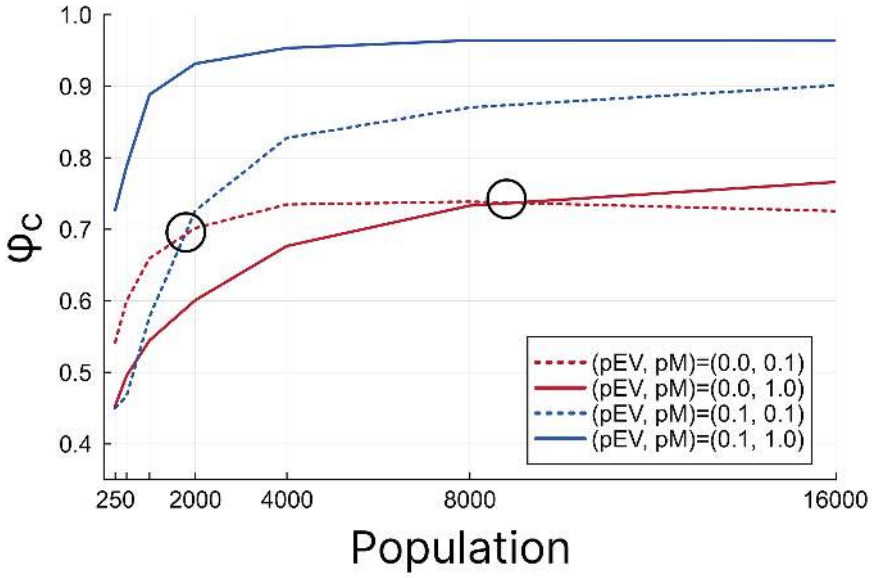

Figure 4.5: Influence of population size (N) on cooperation rate (ϕ_C). The figure shows two crossovers: at $N \approx 2000$ between $(p_{EV}, p_M) = (0.0, 0.1)$ (red dashed) and $(0.1, 0.1)$ (blue dashed), and at $N \approx 8000$ between $(0.0, 0.1)$ (red dashed) and $(0.0, 1.0)$ (red solid). These crossovers reflect how population size alters the relative benefits of environmental variability and mobility through changes in cooperator encounter rates and spatial resource distribution. Parameter settings: $\phi_C^0 = 0.0$, 2-SoR, $T = 1.2$, $S = -0.2$, $p_{SoR} = 0.1$, $\mu = 0.01$. The results for $N = 32000$ are omitted because they exhibited negligible differences from $N = 16000$.

the effect is less conspicuous than in the 2-SoR setting (Figure 4.6a). In terms of ϕ_C^0, initiation with no cooperators ($\phi_C^0 = 0$) in the 2-SoR configuration results in large defector groups, whereas intermediate or full cooperation ($\phi_C^0 = 0.5$ or 1) maintains the large structure but with a higher cooperator frequency within it (Figure 4.7). Consequently, these conditions mask the significant effects of defector group collapse and cooperator group formation observed in Subsection 4.2.

We also confirmed that changing the distance metric from Euclidean to the Chebyshev or Manhattan distance alters the size and shape of the groups, thereby affecting the results. However, these effects are primarily attributed to differences in the group size rather than the shape. Thus, comparisons among these distance metrics can be interpreted as theoretically equivalent to the comparison between the 1-SoR and 2-SoR settings. Essentially, the formation of large defector groups in stable environments is the critical prerequisite for the results described in Subsection 4.2.

SoR orientation

SoR orientation (p_{SoR}) noticeably influences the cooperation rate (Figure 4.8). Increasing p_{SoR} from 0 to 0.1 improves cooperation rates by approximately 20%–40% if $p_{EV} > 0$. However, further increases in p_{SoR} beyond 0.2 reduce the cooperation rate. This reduction occurs be-

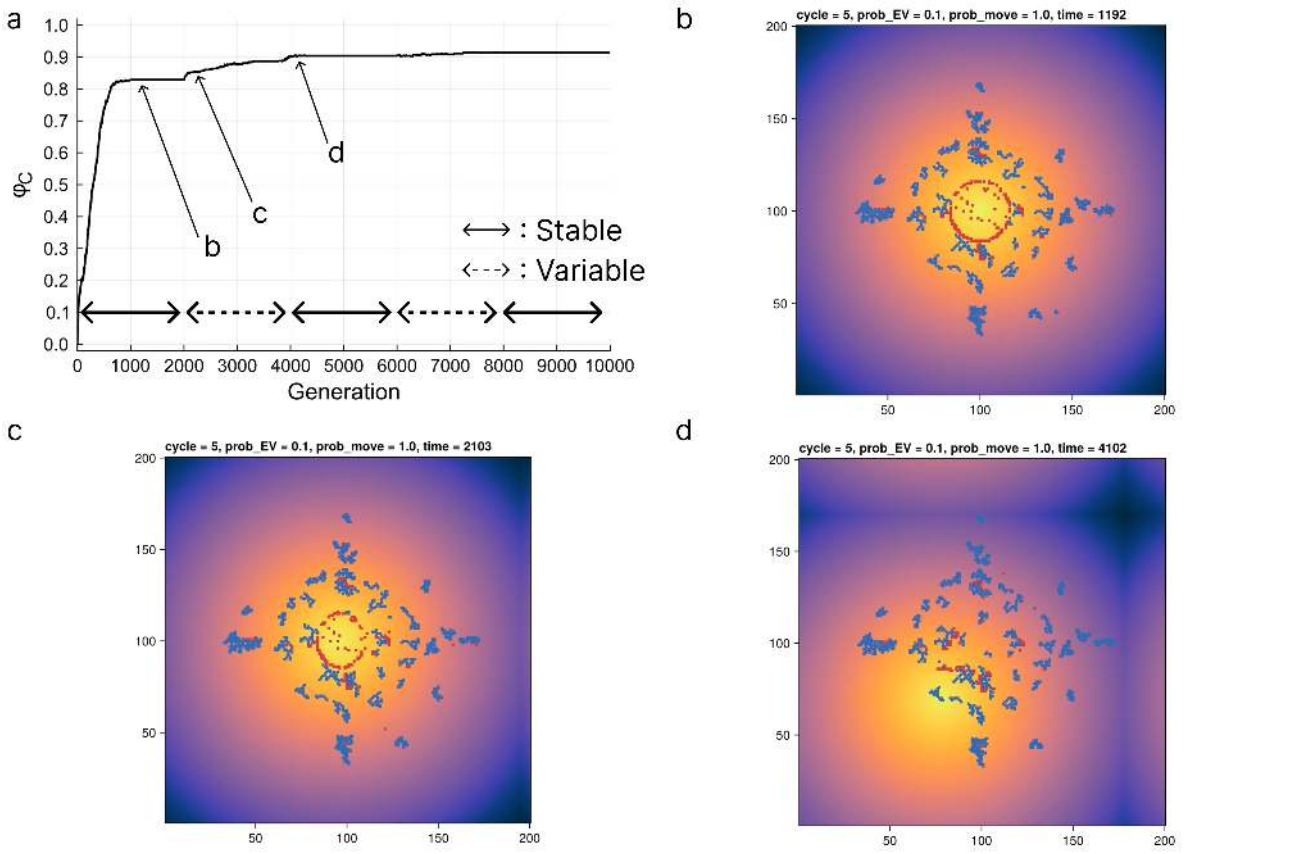

Figure 4.6: Temporal dynamics under cyclic environmental variability in the 1-SoR configuration. The figure shows that the 1-SoR configuration forms only a small circular resource-rich area, resulting in a less pronounced impact of defector group collapse on overall cooperation levels compared to Figure 4.3 (2-SoR). All other parameters and the interpretation of the visual elements are the same as in Figure 4.3.

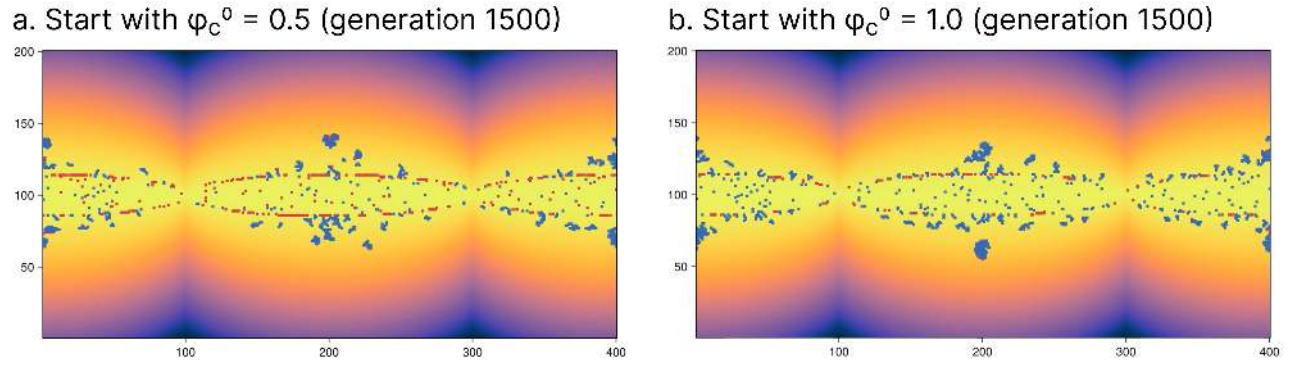

Figure 4.7: Central resource-rich areas under $\phi_C^0 = 0.5$ or 1.0. The figure shows that higher initial cooperation rates maintain larger cooperative structures in resource-rich areas, masking the effects of defector group collapse and cooperator group formation observed with $\phi_C^0 = 0.0$. All parameters (except ϕ_C^0) and the interpretation of the visual elements are the same as in Figure 4.3.

cause excessive p_{SoR} increases the likelihood of agent collisions, which in turn hinders effective migration. These findings suggest that some randomness in the agent mobility is required to maintain a high level of cooperation.

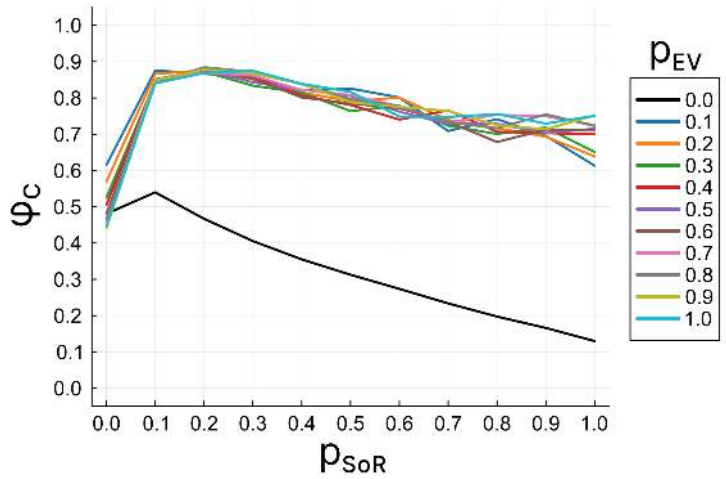

Figure 4.8: Influence of SoR orientation (p_{SoR}) on the cooperation rate (ϕ_C). The figure shows that moderate SoR orientation ($p_{SoR} \approx 0.1$) maximally promotes cooperation, while excessive p_{SoR} reduces cooperation due to increased agent collisions that hinder effective migration. Parameter settings: $N = 1000$, $\phi_C^0 = 0.0$, 2-SoR, $p_M = 1.0$, $T = 1.2$, $S = -0.2$, $\mu = 0.01$.

Payoff parameters and mutation rate

We also investigated the effects of varying the values of the payoff parameters (T, S) across several game structures and the mutation rate μ (including $\mu = 0$ and $\mu = 0.01$). While these variations did not yield qualitatively new insights, they confirmed the robustness of the observed patterns. For completeness, the corresponding results are provided in the Appendix.

4.3 Summary

In this chapter, we examined the joint effects of environmental variability and agent mobility on the evolution of cooperation to understand the causal dynamics of these factors in spatially structured populations. The model incorporates unpredictable environmental variability by implementing SoRs that move randomly across a 2D space, generating dynamic spatial heterogeneity in resource availability. Agents accumulate resources through cooperative or competitive interactions, and the agents with lower resource levels are more likely to migrate to neighboring cells and update their strategies. With this model, we identified three key findings. First, with sufficient agent mobility, even modest environmental variability promotes cooperation; however, further variability does not enhance cooperation. Second, with any level of environmental variability, agent mobility promotes cooperation. Third, these effects occur because environmental variability disrupts a few large stable defector groups that form in resource-rich areas, and agent mobility effectively enables the formation of numerous small cooperator groups at those sites.

Chapter 5

Conclusion

5.1 Summary and cross-model comparison

This dissertation investigated whether and how environmental variability (EV) promotes the evolution of cooperation through three distinct modeling approaches.

[TODO: Summarize key findings and mechanisms from Chapter 2]

[TODO: Summarize key findings and mechanisms from Chapter 3]

[TODO: Summarize key findings and mechanisms from Chapter 4]

[TODO: Summarize common and divergent findings across the three models, and the reasons].

[TODO: Summarize common and divergent mechanisms across the three models, and the reasons]

5.2 Implications and significance

The results of this dissertation have several implications for understanding the evolution of cooperation and human behavior.

First, our research extends the variability selection hypothesis (VSH) beyond individual cognitive adaptations. EV during the Middle Stone Age (MSA) has been primarily understood as a selective pressure on individual-level cognitive abilities, particularly brain expansion. Our research demonstrates that EV may have also directly influenced group-level social structures, extending the scope of VSH to encompass collective behavioral patterns. [TODO: Elaborate this paragraph]

Second, this dissertation identifies variability selection as a previously underexplored mechanism in cooperation theory. While numerous mechanisms for the evolution of cooperation have been proposed, variability selection has received limited attention as a potential driver of cooperation. Our findings demonstrate that variability selection can promote cooperation. [TODO: Elaborate this paragraph]

Third, the theoretical insights from this research may inform future empirical work in evolutionary anthropology and archaeology. [TODO: Elaborate this paragraph]

5.3 Limitations and future directions

While this dissertation provides insights into the relationship between EV and cooperation, several limitations warrant acknowledgment and suggest directions for future research.

First, our theoretical findings lack direct empirical validation. Cooperative behaviors leave limited archaeological traces, making it challenging to test predictions against paleoenvironmental and archaeological data. Future empirical work integrating paleoclimatic records with archaeological evidence of social organization and resource sharing could test whether cooperation patterns correlate with periods of environmental variability. [TODO: Elaborate this paragraph.]

Second, the models employed in this research are too simple as representations of reality. The spatial structures, migration patterns, interaction mechanisms, and strategy updating rules could be modeled in numerous alternative ways. While the three modeling approaches serve as appropriate starting points, they are far from exhaustive, and substantial room remains for developing more diverse and realistic models. [TODO: Elaborate this paragraph.]

Third, the models are too complex for full analytical treatment. The three models examined in this dissertation incorporate sufficient detail to capture realistic dynamics but are consequently difficult to analyze mathematically. Future research could benefit from developing simpler, analytically tractable models that isolate key mechanisms identified in this work. [TODO: Elaborate this paragraph.]

Appendix

Appendix for Chapter 2 The base model

All data, as well as the code required to run the simulations and generate the figures, are available at https://github.com/mas178/Inaba2024

Appendix for Chapter 3 The 2-level model with migration

All data, as well as the code required to run the simulations and generate the figures, are available at https://github.com/mas178/Inaba2025-2Lvl

Appendix for Chapter 4 The 2-dimensional model with migration

All data, as well as the code required to run the simulations and generate the figures, are available at https://github.com/mas178/Inaba2025-2D

Bibliography

[1] C. Darwin. On the origin of species. 1859.

[2] C. Darwin. The descent of man, and selection in relation to sex. 1871.

[3] W. Hamilton. The genetical evolution of social behaviour. I. *J. theor. biol.* 7.1 (1964), 1–16. DOI: 10.1016/0022-5193(64)90038-4.

[4] W. D. Hamilton. The genetical evolution of social behaviour. II. *J. theor. biol.* 7.1 (1964), 17–52. DOI: 10.1016/0022-5193(64)90039-6.

[5] M. A. Nowak, C. E. Tarnita, and E. O. Wilson. The evolution of eusociality. *Nature* 466.7310 (2010), 1057–1062. DOI: 10.1038/nature09205.

[6] P. Abbot, J. Abe, J. Alcock, S. Alizon, J. A. C. Alpedrinha, M. Andersson, et al. Inclusive fitness theory and eusociality. *Nature* 471.7339 (2011), E1–4, author reply E9–10. DOI: 10.1038/nature09831.

[7] M. van Veelen. The general version of hamilton's rule. *Elife* (2025). DOI: 10.7554/elife.105065.1.

[8] J. M. Smith and G. R. Price. The logic of animal conflict. *Nature* 246.5427 (1973), 15–18. DOI: 10.1038/246015a0.

[9] R. Axelrod and W. D. Hamilton. The evolution of cooperation. *Science* 211.4489 (1981), 1390–1396. DOI: 10.1126/science.7466396.

[10] M. A. Nowak and K. Sigmund. Evolution of indirect reciprocity by image scoring. *Nature* 393.6685 (1998), 573–577. DOI: 10.1038/31225.

[11] M. A. Nowak and K. Sigmund. Evolution of indirect reciprocity. *Nature* 437.7063 (2005), 1291–1298. DOI: 10.1038/nature04131.

[12] H. Ohtsuki, C. Hauert, E. Lieberman, and M. A. Nowak. A simple rule for the evolution of cooperation on graphs and social networks. *Nature* 441.7092 (2006), 502–505. DOI: 10.1038/nature04605.

[13] A. Traulsen and M. A. Nowak. Evolution of cooperation by multilevel selection. *Proc. natl. acad. sci. u. s. a.* 103.29 (2006), 10952–10955. DOI: 10.1073/pnas.0602530103.

[14] M. A. Nowak. Five rules for the evolution of cooperation. *Science* 314.5805 (2006), 1560–1563.

[15] S. A. West, A. S. Griffin, and A. Gardner. Evolutionary explanations for cooperation. *Curr. biol.* 17.16 (2007), R661–72. DOI: 10.1016/j.cub.2007.06.004.

[16] S. Mcbrearty and A. S. Brooks. The revolution that wasn't: a new interpretation of the origin of modern human behavior. *J. hum. evol.* 39.5 (2000), 453–563. DOI: 10.1006/jhev.2000.0435.

[17] C. S. Henshilwood and C. W. Marean. The origin of modern human behavior: critique of the models and their test implications. *Curr. anthropol.* 44.5 (2003), 627–651. DOI: 10.1086/377665.

[18] F. d'Errico, A. Pitarch Martí, C. Shipton, E. Le Vraux, E. Ndiema, S. Goldstein, et al. Trajectories of cultural innovation from the middle to later stone age in eastern africa: personal ornaments, bone artifacts, and ocher from panga ya saidi, kenya. *J. hum. evol.* 141.102737 (2020), 102737. DOI: 10.1016/j.jhevol.2019.102737.

[19] J. Wilkins, B. J. Schoville, R. Pickering, L. Gliganic, B. Collins, K. S. Brown, et al. Innovative homo sapiens behaviours 105,000 years ago in a wetter kalahari. *Nature* 592.7853 (2021), 248–252. DOI: 10.1038/s41586-021-03419-0.

[20] A. Bergström, C. Stringer, M. Hajdinjak, E. M. L. Scerri, and P. Skoglund. Origins of modern human ancestry. *Nature* 590 (2021), 229–237. DOI: 10.1038/s41586-021-03244-5.

[21] R. Potts. Evolution and climate variability. *Science* 273.5277 (1996), 922–923. DOI: 10.1126/science.273.5277.922.

[22] R. Potts. Environmental hypotheses of hominin evolution. *Am. j. phys. anthropol.* 107.S27 (1998), 93–136. DOI: 10.1002/(sici)1096-8644(1998)107:27+<93::aid-ajpa5>3.0.co;2-x.

[23] J. T. Faith, A. Du, A. K. Behrensmeyer, B. Davies, D. B. Patterson, J. Rowan, et al. Rethinking the ecological drivers of hominin evolution. *Trends ecol. evol.* 36.9 (2021), 797–807.

[24] C. Schuck-Paim, W. J. Alonso, and E. B. Ottoni. Cognition in an ever-changing world: climatic variability is associated with brain size in Neotropical parrots. *Brain behav. evol.* 71.3 (2008), 200–15. DOI: 10.1159/000119710.

[25] D. Sol, S. Bacher, S. M. Reader, and L. Lefebvre. Brain size predicts the success of mammal species introduced into novel environments. *Am. nat.* 172.S1 (2008), S63–71. DOI: 10.1086/588304.

[26] D. Sol. Revisiting the cognitive buffer hypothesis for the evolution of large brains. *Biol. lett.* 5.1 (2009), 130–3. DOI: 10.1098/rsbl.2008.0621.

[27] M. Grove. Speciation, diversity, and mode 1 technologies: the impact of variability selection. *J. hum. evol.* 61.3 (2011), 306–319.

[28] A. Navarrete, C. P. van Schaik, and K. Isler. Energetics and the evolution of human brain size. *Nature* 480.7375 (2011), 91–93.

[29] M. Will, M. Krapp, J. T. Stock, and A. Manica. Different environmental variables predict body and brain size evolution in homo. *Nat. commun.* 12.1 (2021), 4116.

[30] J. M. Stibel. Climate change influences brain size in humans. *Brain behav. evol.* 98.2 (2023), 93–106.

[31] A. Whiten and R. Byrne. The machiavellian intelligence hypotheses: editorial. in: byrne rw, whiten a, editors. *Machiavellian intelligence: social expertise and the evolution of intellect in monkeys, apes, and humans.* 413 (1988). Ed. by R. W. Byrne, 1–9.

[32] R. I. M. Dunbar. The social brain hypothesis. *Evol anthropol* 6.5 (1998), 178–190.

[33] L. Barrett, P. Henzi, and D. Rendall. Social brains, simple minds: does social complexity really require cognitive complexity? *Philos. trans. r. soc. lond. b biol. sci.* 362.1480 (2007), 561–575.

[34] M. Grove and F. Coward. From individual neurons to social brains. *Camb. archaeol. j.* 18.3 (2008), 387–400.

[35] C. Knight and C. Power. Social conditions for the evolutionary emergence of language. Oxford: Oxford University Press, 2011.

[36] S. C. Hayes and B. T. Sanford. Cooperation came first: evolution and human cognition. *J. exp. anal. behav.* 101.1 (2014), 112–129.

[37] R. I. M. Dunbar. The social brain hypothesis - thirty years on. *Ann. hum. biol.* 51.1 (2024), 2359920. DOI: 10.1080/03014460.2024.2359920.

[38] A. R. DeCasien, S. A. Williams, and J. P. Higham. Primate brain size is predicted by diet but not sociality. *Nat. ecol. evol.* 1.5 (2017), 112.

[39] M. Grabowski, B. T. Kopperud, M. Tsuboi, and T. F. Hansen. Both diet and sociality affect primate brain-size evolution. *Syst. biol.* 72.2 (2023), 404–418.

[40] M. A. Brockhurst, A. Buckling, and A. Gardner. Cooperation peaks at intermediate disturbance. *Curr. biol.* 17.9 (2007), 761–5. DOI: 10.1016/j.cub.2007.02.057.

[41] S. Miller and J. Knowles. Population fluctuation promotes cooperation in networks. *Sci. rep.* 5 (2015), 11054. DOI: 10.1038/srep11054.

[42] C. S. Gokhale and C. Hauert. Eco-evolutionary dynamics of social dilemmas. *Theor. popul. biol.* 111 (2016), 28–42. DOI: 10.1016/j.tpb.2016.05.005.

[43] V. Stojkoski, M. Karbevski, Z. Utkovski, L. Basnarkov, and L. Kocarev. Evolution of cooperation in networked heterogeneous fluctuating environments. *Physica a* 572 (2021), 125904. DOI: 10.1016/j.physa.2021.125904.

[44] D. Kroumi, É. Martin, C. Li, and S. Lessard. Effect of variability in payoffs on conditions for the evolution of cooperation in a small population. *Dyn. games appl.* 11.4 (2021), 803–34. DOI: 10.1007/s13235-021-00383-2.

[45] J. M. Borg and A. Channon. Testing the variability selection hypothesis: the adoption of social learning in increasingly variable environments. *International conference on the simulation and synthesis of living systems* (2012), 317–324.

[46] M. Assaf, M. Mobilia, and E. Roberts. Cooperation dilemma in finite populations under fluctuating environments. *Phys. rev. lett.* 111 (2013), 238101. DOI: 10.1103/PhysRevLett.111.238101.

[47] M. Pereda, D. Zurro, J. I. Santos, I. Briz I Godino, M. Álvarez, J. Caro, et al. Emergence and evolution of cooperation under resource pressure. *Sci. rep.* 7 (2017), 45574. DOI: 10.1038/srep45574.

[48] A. Szolnoki and X. Chen. Environmental feedback drives cooperation in spatial social dilemmas. *Epl* 120 (2017), 58001. DOI: 10.1209/0295-5075/120/58001.

[49] J. Huang, Y. Zhu, D. Zhao, C. Xia, and M. Perc. The impact of feedbacks on evolutionary game dynamics in structured populations. *Chaos* 35.6 (2025), 063134. DOI: 10.1063/5.0278673.

[50] M. Inaba and E. Akiyama. Environmental variability promotes the evolution of cooperation among geographically dispersed groups on dynamic networks. *Plos complex syst.* 2.4 (2025), e0000038. DOI: 10.1371/journal.pcsy.0000038.

[51] D. W. Bird, R. B. Bird, B. F. Codding, and D. W. Zeanah. Variability in the organization and size of hunter-gatherer groups: foragers do not live in small-scale societies. *J. hum. evol.* 131 (2019), 96–108.

[52] R. I. M. Dunbar. Structure and function in human and primate social networks: implications for diffusion, network stability and health. *Proc. math. phys. eng. sci.* 476.2240 (2020), 20200446.

[53] J. M. Smith. Group selection. *Q. rev. biol.* 51.2 (1976), 277–283.

[54] S. Okasha. Why won't the group selection controversy go away? *Br. j. philos. sci.* 52.1 (2001), 25–50.

[55] O. T. Eldakar and D. S. Wilson. Eight criticisms not to make about group selection. *Evolution* 65.6 (2011), 1523–1526.

[56] C. K. W. De Dreu and Z. Triki. Intergroup conflict: origins, dynamics and consequences across taxa. *Philos. trans. r. soc. lond. b biol. sci.* 377.1851 (2022), 20210134.

[57] A. M. M. Rodrigues, J. L. Barker, and E. J. H. Robinson. The evolution of intergroup cooperation. *Philos. trans. r. soc. lond. b biol. sci.* 378.1874 (2023), 20220074.

[58] C. W. Marean. Pinnacle Point Cave 13B (Western Cape Province, South Africa) in context: the Cape floral kingdom, shellfish, and modern human origins. *J hum evol* 59.3-4 (2010), 425–443.

[59] L. Wadley, C. Sievers, M. Bamford, P. Goldberg, F. Berna, and C. Miller. Middle stone age bedding construction and settlement patterns at Sibudu, South Africa. *Science* 334.6061 (2011), 1388–1391.

[60] A. W. Kandel and N. J. Conard. Settlement patterns during the earlier and Middle stone age around Langebaan Lagoon, western Cape (South Africa). *Quat int* 270 (2012), 15–29.

[61] K. Hasselmann. Stochastic climate models: Part I. Theory. *Tellus a* 28.6 (1976), 473–485.

[62] D. Vyushin, P. Kushner, and F. Zwiers. Modeling and understanding persistence of climate variability. *J geophys res* 117.D21 (2012).

[63] S. Salcedo-Sanz, D. Casillas-Pérez, J. Del Ser, C. Casanova-Mateo, L. Cuadra, M. Piles, et al. Persistence in complex systems. *Phys rep* 957 (2022), 1–73.

[64] G. Hardin. The tragedy of the commons: the population problem has no technical solution; it requires a fundamental extension in morality. *Science* 162.3859 (1968), 1243–1248.

[65] K. G. Binmore. Game theory and the social contract: just playing. Vol. 2. Cambridge: MIT Press, 1994.

[66] P. Kollock. Social dilemmas: the anatomy of cooperation. *Annu. rev. sociol.* 24 (1998), 183–214. DOI: 10.1146/annurev.soc.24.1.183.

[67] F. C. Santos, M. D. Santos, and J. M. Pacheco. Social diversity promotes the emergence of cooperation in public goods games. *Nature* 454.7201 (2008), 213–216.

[68] F. C. Santos and J. M. Pacheco. Scale-free networks provide a unifying framework for the emergence of cooperation. *Phys. rev. lett.* 95.9 (2005), 098104.

[69] F. C. Santos, J. M. Pacheco, and T. Lenaerts. Evolutionary dynamics of social dilemmas in structured heterogeneous populations. *Proc. natl. acad. sci. u. s. a.* 103.9 (2006), 3490–3494.

[70] Y. Meng, S. P. Cornelius, Y.-Y. Liu, and A. Li. Dynamics of collective cooperation under personalised strategy updates. *Nat. commun.* 15.1 (2024), 3125.

[71] M. Inaba and E. Akiyama. Evolution of cooperation among migrating resource-oriented agents under environmental variability. *Chaos, solitons & fractals* 202 (2025), 117592. DOI: 10.1016/j.chaos.2025.117592.

[72] L. A. Dugatkin and D. S. Wilson. Rover: a strategy for exploiting cooperators in a patchy environment. *Am. nat.* 138.3 (1991), 687–701. DOI: 10.1086/285243.

[73] M. H. Vainstein, A. T. C. Silva, and J. J. Arenzon. Does mobility decrease cooperation? *J. theor. biol.* 244.4 (2007), 722–8. DOI: 10.1016/j.jtbi.2006.09.012.

[74] R. Cong, B. Wu, Y. Qiu, and L. Wang. Evolution of cooperation driven by reputation-based migration. *Plos one* 7.5 (2012), e35776. DOI: 10.1371/journal.pone.0035776.

[75] X. Chen, A. Szolnoki, and M. Perc. Risk-driven migration and the collective-risk social dilemma. *Phys. rev. e* 86 (2012), 036101. DOI: 10.1103/PhysRevE.86.036101.

[76] Z. He, Y. Geng, C. Shen, and L. Shi. Evolution of cooperation in the spatial prisoner's dilemma game with extortion strategy under win-stay-lose-move rule. *Chaos solitons fractals* 141 (2020), 110421. DOI: 10.1016/j.chaos.2020.110421.

[77] S. Dhakal, R. Chiong, M. Chica, and R. H. Middleton. Climate change induced migration and the evolution of cooperation. *Appl. math. comput.* 377 (2020), 125090. DOI: 10.1016/j.amc.2020.125090.

[78] T. Ren and J. Zheng. Evolutionary dynamics in the spatial public goods game with tolerance-based expulsion and cooperation. *Chaos solitons fractals* 151 (2021), 111241. DOI: 10.1016/j.chaos.2021.111241.

[79] Y. Yang, Q. Pan, and M. He. The influence of environment-based autonomous mobility on the evolution of cooperation. *Chaos solitons fractals* 169 (2023), 113320. DOI: 10.1016/j.chaos.2023.113320.

[80] H. Zhang. Evolution of cooperation among fairness-seeking agents in spatial public goods game. *Appl. math. comput.* 489 (2025), 129183. DOI: 10.1016/j.amc.2024.129183.

[81] B. A. Huberman and N. S. Glance. Evolutionary games and computer simulations. *Proc. natl. acad. sci. u.s.a.* 90.16 (1993), 7716–8. DOI: 10.1073/pnas.90.16.7716.

[82] G. Zhang, X. Xiong, B. Pi, M. Feng, and M. Perc. Spatial public goods games with queueing and reputation. *Appl. math. comput.* 505 (2025), 129533. DOI: 10.1016/j.amc.2025.129533.

Acknowledgments